NTNU
Norwegian University of
Science and Technology

Oxidation of methanol to formaldehyde over Ag catalyst

A study of reaction pathways and Ag catalyst restructuring during MTF

Kamilla Arnesen

Chemical Engineering and Biotechnology
Submission date: June 2018
Supervisor: Hilde Johnsen Venvik, IKP

Norwegian University of Science and Technology
Department of Chemical Engineering

Preface

This thesis concludes my degree in Chemical Engineering at the Norwegian University of Science and Technology (NTNU). This thesis has been the continuum of the work done during the Specialization Project of Fall 2017.

First, I would like to show my gratitude towards my supervisor professor Hilde J. Venvik. Your advise, guidance and enthusiasm has been very much appreciated. I would also like to thank my co-supervisor and associate professor Jia Yang and senior scientist at SINTEF, Rune Lødeng for good discussions and all your help. Big thanks to Ph.D. student Stine Lervold for your support, patience and sparkling mood. This work would not have been the same without you.

I would also like to extend my appreciation towards the great people at the Catalysis department for help and training, in addition to the iCSI partners, Dynea and K.A. Rasmussen for letting me come and visit and making this work more exciting.

Finally, I would like to thank my friends and family for encroachment and support during my years of studying.

Declaration of compliance

I declare that this is an independent work according to the exam regulations at the Norwegian University of Science and Technology.

Kamilla Arnesen

Trondheim, Norway
June 18, 2018

Abstract

Formaldehyde is recognised as an important industrial chemical, being a versatile organic molecule. Due to high reactivity, it is used as a building block to synthesise other chemicals and industrial products. Production of formaldehyde is mainly based on two reactions, dehydrogenation and partial oxidation of methanol. Silver can be used as a catalyst and the technology is recognised by Dynea AS as the process method with most potential for competitive development, based on market and environmental considerations

In this master thesis silver catalyst morphology, activity and interaction between silver and various components relevant to the formaldehyde synthesis have been studied. The catalytic morphology was investigated for dependency on different atmospheres, exposure time and process variables. Catalytic activity was measured for hydrogen, carbon monoxide and, to an extent, methanol oxidation reactions, in addition to focusing on structure dependencies. The catalyst was characterised with XRD and SEM.

Polycrystalline silver catalyst was treated with various atmospheres, such as nitrogen, hydrogen, air and methanol/water, at elevated temperatures. It was also used as the catalyst in oxidation reactions, performed with varying temperatures, to investigate the levels of reactant conversion.

It was found that treating the silver with different atmospheres resulted in great changes of the silver surface and morphology. Structural changes in the silver was observed when oxygen was present. Silver particles treated in air showed increasing restructuring with time, eliminating angular grain structure, production of pinholes and promoting irregular and smooth facet formation. Using the silver as a catalyst for hydrogen, carbon monoxide and methanol oxidation resulted in the same observations. Equal morphological changes were observed on the mesoscale, for silver used as catalyst in hydrogen and carbon monoxide oxidation. The catalyst display high catalytic activity for hydrogen oxidation, increasing with time. A declining trend was evident for catalytic activity for carbon monoxide oxidation, suggesting the restructured silver promotes hydrogen oxidation, as opposed to carbon monoxide oxidation. In general, oxygen display an important role promoting and activating reactions and influence the silver catalyst morphology. This is especially critical for silver catalyst activation and performance during process start-up in the formaldehyde production.

Sammendrag

Formaldehyd er et allsidig organisk molekyl og er ansett som et viktig industrielt kjemikalie. Grunnet dens høye reaktivitet blir det brukt som grunnstein for å syntetiseres andre kjemikalier og industrielle produkter. Produksjonen av formaldehyd er i all hovedsak produsert ved hjelp av to reaksjoner, dehydrogenisering og delvis oksidasjon av metanol. Sølv blir gjerne bukt som katalysator for reaksjonene og er identifisert av Dynea As som den teknologien med størst potensial for konkurransedyktig utvikling basert på økonomisk og miljømessige betrakninger.

Denne masteroppgaven fokuseres det på sølvkatalysatorens morfologi, aktivitet og interaksjonen mellom sølvet og komponenter relevant for produksjonen av formaldehyd. Katalysatorens morfologi var undersøkt i sammenheng med ulike atmosfærer, eksponeringstid og prosessvariabler. Katalytisk aktivitet ble målt for hydrogen, karbonmonoksid, og til delvis, for oksidasjon av metanol. Det ble i tillegg fokusert på reaksjonens strukturavhengighet. Katalysatoren ble karakterisert ved hjelp av XRD og SEM.

Polykrystalinsk sølvkatalysator ble utsatt for ulike atmosfærer som, nitrogen, hydrogen, luft og metanol/vann-blanding, ved høye temperaturer. Sølvet ble også brukt som katalysator for oksidajonsreaksjoner som ble utført ved varierende temperarurer for å undersøke omsetningsgrad.

Resultatene viste at behandling av sølvet ved ulike atmosfærer gjorde store utslag for sølvets morfologi. Strukturelle endringer i sølvet ble observert ved tilstedeværelse av oksygen. Behandling med luft over lengre tid førte til økende restrukturering. Skarp kornstruktur forsvant, hull og uregelmessige falsetter ble dannet. De samme morfologiske forandringene ble observert i sølv som ble brukt som katalysator for hydrogen, karbonmonoksid og metanol oksidasjon. Katalysatoren viste høy katalytisk aktivitet for oksidasjon av hydrogen som økte med eksponeringstiden. En nedadgående trend ble sett for den katalytiske aktiviteten for oksidasjon av karbonmonoksid. Dette tyder på at sølvets restrukturering fremmer oksidasjon av hydrogen, i motsetning til karbonmonoksid. Generelt viser oksygen en viktig egenskap ved å promotere og aktivere reaksjoner, samt påvirke sølvkatalysatorens morfologi. Dette er spesielt viktig for aktivering av sølvkatalysatoren og dens prestasjon ved oppstart av formaldehydproduksjon.

Table of Contents

List of Tables

List of Figures

Abbreviations

BSE	=	Backscattered Electrons
CEM	=	Controlled Evaporation and Mixing
CO	=	Carbon Monoxide
EDX	=	Energy Dispersed X-ray
FCC	=	Face Centred Cubic
GC	=	Gas Chromatoraph
H_2	=	Hydrogen
HSE	=	Health, Safety and Environment
LFC	=	Liquid Flow Controller
MeOH	=	Methanol
MFC	=	Mass Flow Controller
MTF	=	Methanol to Formaldehyde
NTNU	=	Norwegian University of Science and Technology
SE	=	Secondary Electrons
SEM	=	Scanning Electron Microscopy
TCD	=	Thermal Conductive Detector
TOF	=	Turnover Frequency
TOS	=	Time on Stream
TPD	=	Temperature Programmed Desorption
XRD	=	X-Ray Diffraction

Chapter 1

Introduction

Formaldehyde is recognised as an important industrial chemical with a yearly production of 29 million tons (2010) [1]. It is a versatile organic molecule and due to high reactivity, it is used as a building block to synthesise other chemicals and industrial products. Some products are resins for wood panel industry, polyacetal and other acetylenic chemicals making it important for construction, automotive, and the pharmaceutical industry [2].

Formaldehyde production has a long history and was knowingly first synthesised by hydrolysing methylene acetate in 1859. Production went from small to industrial scale after 1923 as a result of the high-pressure synthesis of methanol by BASF [3]. Since then, formalin production, formaldehyde dissolved in water, has expanded by focusing on process and reaction efficiency [2].

Today, two process technologies dominate and account for the majority of formaldehyde production. Initially, a gauze made of silver wires were used as a catalyst, which later have been replaced with a shallow catalyst bed made of silver crystals where methanol is feed in excess with oxygen and H_2O at 600 - 680 °C. Continued development have resulted in the use of iron oxide-molybdenum oxide catalyst. This process operates with excess air and a near complete conversion of methanol at 270 - 400 °C [2].

Based on market and environmental considerations, the silver catalyst technology has been recognised by Dynea AS as the process method with most potential for competitive development [4].

As a way to develop the formaldehyde process, several aspects are under investigation, one being to increase the understanding behind the reactions and catalytic system. Side reactions, gas phase reactions, changes in catalyst morphology and activity are among some of the challenges. This project aims to focus on reaction pathways, the silver catalyst and contribute to the investigation of the interaction between silver and various components present in the formaldehyde synthesis.

Chapter 2

Theory

2.1 Formaldehyde Production by Silver Catalyst

Producing formaldehyde from methanol accounts for about a third of the worlds methanol consumption. The synthesis is mainly based on two reactions shown in Equations 2.1 and 2.2. The former, dehydrogenation, is endothermic, while the latter, partial oxidation, is exothermic [5].

$$CH_3OH \rightleftharpoons CH_2O + H_2 \qquad \Delta H = 84\,\text{kJ/mol} \tag{2.1}$$

$$CH_3OH + \frac{1}{2}O_2 \longrightarrow CH_2O + H_2O \qquad \Delta H = -159\,\text{kJ/mol} \tag{2.2}$$

The two reactions can be carried out simultaneously over a silver catalyst bed at atmospheric pressure and temperatures of 600 - 680 °C, where the exothermic partial oxidation reaction supplies heat to the dehydrogenation. Several side reactions also takes place producing carbon dioxide, methyl formate and formic acid. Carbon dioxide can be produced by complete oxidation of methanol shown in Equations 2.3 and 2.6.

Typically methanol, air and water are mixed and evaporated in a vaporiser and heated to reaction temperature before being fed to the reactor. The reaction occur on a silver catalyst bed (10 - 50 mm). To avoid product decomposition, the product gas is cooled directly after the reactor in a waste heat boiler and fed to an absorber. Water is mixed in to stabilise the product and yield formalin (37 wt% formaldehyde in water). Formaldehyde is an unstable chemical and can polymerise easily. Methanol (3 - 12 wt%) is added to the formalin solution as an inhibitor for this purpose. It is also important to minimise formic acid content to increase product quality. The formaldehyde synthesis is run at adiabatic conditions, making temperature control important. Methanol is recycled and fed in excess

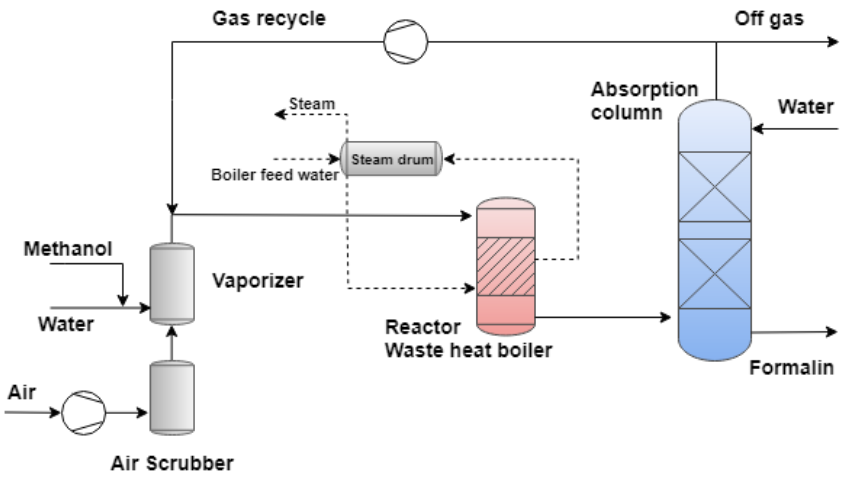

Figure 2.1: Illustration of the methanol to formaldehyde process using silver catalyst at Dynea.

for this purpose, in addition to avoid operating in the explosive methanol - air area [5]. This process can yield a near complete methanol conversion with about 90 - 92 % selectivity towards formaldehyde [6] and is illustrated in Figure 2.1.

Silver catalyst is operational from a few months to a year before regeneration is needed, which usually is done by electrolysis. A common reason for decreasing catalytic performance is sintering, which happen at high reaction temperatures, and poisoning, such as iron. Water is generally added to the feed at a methanol/water 60/40 weight ratio. It is often called *water ballast process* and is shown to increase the catalyst lifetime by distributing the heat across the catalyst bed and lower the risk of sintering and coke poisoning. Coke can be produced by methanol decomposing to carbon, water and hydrogen as shown in Equation 2.4. As the risk of overheating is lowered with adding water to the feed, the oxygen concentration can be increased, improving the conversion and yield [3].

$$CH_3OH + \frac{3}{2}O_2 \longrightarrow CO_2 + 2\,H_2O \qquad \Delta H = -\,674\,\text{kJ/mol} \tag{2.3}$$

$$CH_3OH \longrightarrow C + H_2O + H_2 \qquad \Delta H = -\,31\,\text{kJ/mol} \tag{2.4}$$

Qian et al. have performed a study comparing formaldehyde synthesis with and without water in the feed. The goal was to investigate the effect of water on the catalyst, formaldehyde selectivity and study the effect it had on the production of byproducts. The research concluded that adding water to the reaction feed increased the methanol conversion and gave a better selectivity towards formaldehyde [7]. In addition, it reduced the formation of the byproduct formic acid, which is unwanted as it is a corrosive acid and will contribute to polymerisation of formaldehyde [7, 2]. Formaldehyde is an unstable chemical and can decompose at high temperatures to H_2 or CO, oxidise to CO_2 and H_2O or formic acid

in the presence of oxygen, as shown in Equations 2.5 to 2.7. The complete oxidation of formaldehyde and formation of formic acid are strongly exothermic reactions which may produce local hot spots and sintering of the catalyst [7].

$$CH_2O \longrightarrow CO + H_2 \qquad \Delta H = 12\,\text{kJ/mol} \tag{2.5}$$

$$CH_2O + O_2 \longrightarrow CO_2 + H_2O \qquad \Delta H = -514\,\text{kJ/mol} \tag{2.6}$$

$$CH_2O + \frac{1}{2}O_2 \longrightarrow HCOOH \qquad \Delta H = -314\,\text{kJ/mol} \tag{2.7}$$

In addition to increase the catalyst lifetime, water can also influence catalyst activity [3]. Bao et al. investigated the effect of water on bonds created on a silver (111) surface discovering correlations between promotion of surface restructuring and the formation of oxygen species active in the formaldehyde synthesis, promoting formaldehyde selectivity [8].

Oxygen in the feed is primarily used by the exothermic reactions in Equation 2.2 and to some extent in Equations 2.3 and 2.6. By adjusting air in the feed, the reactor and catalyst bed temperature vary, controlling to what extent the endothermic reactions occur, in Equations 2.1 and 2.5. The reaction in Equation 2.5 is not a desired reaction and shows the importance of cooling the product stream after the reactor [2]. Waterhouse et al. concluded with an ideal methanol/oxygen feed ratio of 2.25 when studying industrial formaldehyde manufacturing with a focus on examining the role of oxygen species in methanol oxidation on silver [9].

2.1.1 Interaction of Oxygen with Silver

A complete reaction mechanism for the formaldehyde synthesis is still not known and several theories exist. The two main theories will be mentioned further.

Wachs and Madix performed experiments using isotopic labelling showing absorbed atomic oxygen must be present to promote methoxy, formaldehyde and formate species and created a subsequent reaction mechanism [10]. Andreasen et al. used this model as a basis when developing a microkinetic model for oxidation of methanol to formaldehyde and oxidation of formaldehyde to carbon dioxide [11]. They argued only one type of atomic oxygen, O_α, is active in the formaldehyde synthesis and based the model on a consecutive reaction path and kinetic calculations.

Researchers have also studied the interactions between oxygen and silver with regards to the formaldehyde synthesis to explain the reaction mechanism [9, 12, 13]. Three species of atomic oxygen have been identified as O_α, O_β and O_γ. The oxygen species exhibit different properties and behaviour with regards to silver interactions and formaldehyde formation, as illustrated in Figure 2.2. O_α is agreed to be chemisorbed atomic oxygen

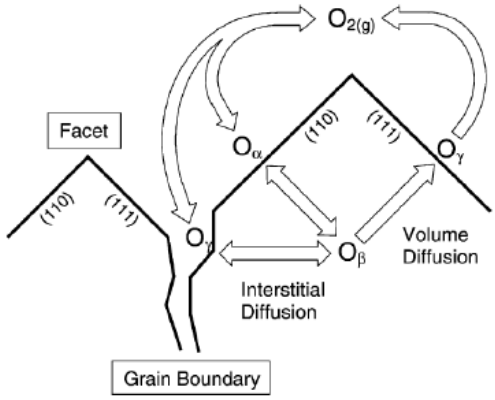

Figure 2.2: Illustration of the interactions of various oxygen species with silver catalyst at 923 K. Figure is obtained from [13]

species creating bridge bonds (Ag-O-Ag) on the silver surface on the low index planes of silver. This oxygen is related to partial oxidation of methanol to formaldehyde and oxidation of methanol and formaldehyde to carbon dioxide and dominates at temperatures lower then 350 °C [12]. At elevated temperatures oxygen may dissolve in the silver bulk and grain boundaries to create O_β, which is associated with surface restructuring of the silver [9]. The last oxygen species, O_γ, is a result of volume diffusion of O_β through the silver bulk at high temperatures, 600 °C, creating strong terminal bonds (Ag=O), which catalyse dehydrogenation of methanol to formaldehyde and hydrogen [7]. Bulk dissolved oxygen reacting with hydrogen creating water is also discussed to be the source of hole formation in the catalyst surface [14].

Even though oxygen is not directly involved in all reactions creating formaldehyde it is an important factor in the conversion of methanol and formaldehyde yield, as discovered by Qian et al. During a 300 days MTF experiment the catalyst was temporarily exposed to an oxygen-free atmosphere from steady-state. When the normal oxygen feed returend an decrease in methanol conversion and a shift in selectivity towards carbon dioxide and formic acid was observed, associating this behaviour with an increased amount of the the weakly bound atomic O_α on the silver surface [7].

2.1.2 Oxidation of Hydrogen and Carbon Monoxide

According to the industrial review by Millar and Collins, there is still much to understand and learn to improve the industrial production of formaldehyde. Some of the concluding remarks concerning improvements were about process optimisation and eliminating silver poisons to expand the catalyst lifetime [3]. This would include obtaining a greater understanding of the reaction pathways and production of byproducts.

Two of these products are water and carbon dioxide. Production of water and carbon

dioxide are included in several reactions previously shown, and are suggested signs of reactant and product decomposition. The amount of water can also indicate which of the reaction pathways dominate and produce formaldehyde (dehydrogenation or partial oxidation of methanol). For the production of formaldehyde it is naturally most beneficial to maximise the production of the desired product and minimise byproducts. It is also of interest to understand the source and the amount being produced of byproducts to indicate to what extent methanol combustion and formaldehyde decomposition occur during the reaction [3].

Deactivation of silver, as mentioned, is caused by poisons and sintering. A suspected cause of sintering is the presence of water vapour at elevated temperatures and as a result of deactivation the increased selectivity towards the byproducts carbon dioxide and formic acid occur [6, 14]. In addition to the role of oxygen acting as a promoter of silver surface reconstruction, a study by Millar et al. suggest the production of water and carbon dioxide by oxidation can be the cause of pinhole formation in the silver surface [14].

Qu et al. performed experiments concluding with oxygen pretreated silver exhibit good activity towards the oxidation of carbon monoxide at room temperature, suggesting carbon dioxide could be a product from carbon monoxide oxidation [15]. The activity at higher temperatures are not certain. Work by Van Santen state that recombination of adsorbed oxygen and CO to CO_2 occurs on most transition metal surfaces, but have a maximum rate as a function of temperature and CO surface coverage. The reaction rate increase with temperature to the point where the adsorption equilibrium of CO is shifted towards the gas phase. Experiments have also been performed with single surface Pt crystal, which stabilise the structure by shifting from (100) to (111) structure, in a vacuum. The absorption of CO activate the surface towards creating a more reactive (100) surface, promoting CO_2 formation. Desorption of the product promote surface restructuring toward the stable (111) structure and a oscillatory behaviour [16].

If the silver surface is active for oxidation of hydrogen and carbon monoxide, these reactions are competing for consumption of oxygen. The exothermic oxidation reactions are shown in Equations 2.8 and 2.9.

$$H_2 + \frac{1}{2} O_2 \longrightarrow H_2O \qquad \Delta H = -243\,\text{kJ/mol} \tag{2.8}$$

$$CO + \frac{1}{2} O_2 \longrightarrow CO_2 \qquad \Delta H = -283\,\text{kJ/mol} \tag{2.9}$$

2.2 Silver Catalyst

In heterogeneous catalysis the common interface is that between solid and gas. The chemical reaction occur on said surface on active catalytic sites. The surface can exhibit local variations resulting in individual site reactivity. These sites can activate the reactant differently and based on the geometry of the site, the interaction can result in different adsorbed

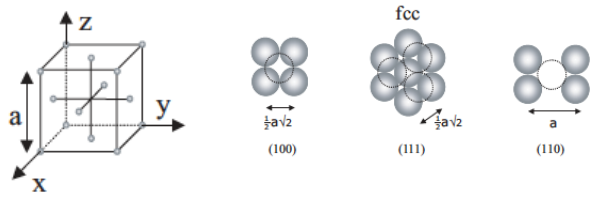

Figure 2.3: Illustration of a fcc unit cell (left) and basal plane structures (100), (111) and (110) (right). Stippled lines in figure to the right indicate the second layer atom locations and a is the lattice constant determining the distance between atoms. The figures are obtained from [18].

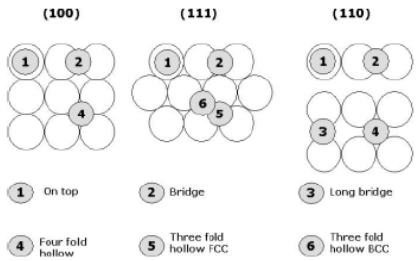

Figure 2.4: Illustration of on-top, bridge and hollow adsorption sites on fcc structure. The figure is obtained from [18].

states on the metal surface. These states are important because it is the interaction between molecule and active site that decide which bonds are broken and created making product selectivity the result of molecule activation. Metallic surfaces also effect the formation of molecular states in the absorbate making the basal plane structure and orbital interactions a factor which also determine reactivity and product formation [17].

Silver is a frequently used catalyst with a face-centred cubic crystal structure (fcc), which is one of the closest packed spheres with only 26 % empty space. For cubic structures the main basal planes are (100), (110) and (111), as defined by Miller indices. The fcc structure and illustration of the basal planes are shown in Figure 2.3, where the broken lines indicate the second layer of atoms and a is the lattice constant determining the distance between atoms [18] .

Metal surface atoms change their bonding geometry to adapt to not having a complete set of nearest amtomic neighbours, resulting in different properties than atoms in the bulk material. The number of unsaturated bonds and increased energy level effect the activity of a site on the catalyst resulting in different adsorption sites. Some of the most common sites are illustrated in Figure 2.4, showing the geometry of on-top, bridge and hollow sites on the fcc structure. Complex surfaces also contain defects, such as steps, kinks, terraces, adatoms and vacancies, which are illustrated in Figure 2.5. Due to the different energy levels some bonds are more likely to be broken at step and kink sites then at terraces [19]. In polycrystalline materials, composed of small crystals or grains, the grain boundary create an interface similar to the surface with increased surface energy and reactivity. An

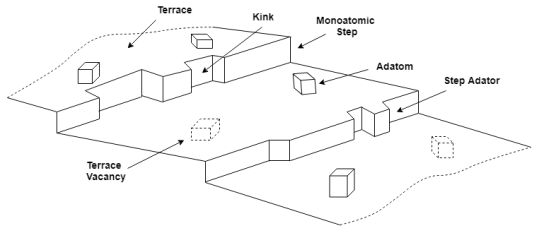

Figure 2.5: Sketch of a heterogeneous solid surface showing various surface sites. The figure is inspired by [17].

example of a grain boundary in polycrystalline silver is illustrated in Figure 2.2 [20].

When a surface is created, bonds may be broken, resulting in increased surface free energy. Some surface processes and phenomenons are therefore a result of minimising the surface free energy, such as creating a dense packed surface, maximising the amount of nearest neighbours and keeping impurities at the surface [18]. The minimum energy configuration for silver is the closed packed (111) structure. Facet formation require atom mobility to reconstruct both surface and bulk material and occur more easily at temperatures above 345 °, which is the Tammann temperature for silver. The Tammann temperature is defined as the temperature where the atoms has gained sufficient thermal energy to clearly notice increased bulk mobility and activity [13].

With regards to the formaldehyde process it is known that the silver morphology effects the reactivity and methanol selectivity towards formaldehyde, especially during the start-up period of the process. Electrolytic silver vary in shape, size, surface area, exposed plains and defects depending on supplier. These variations effect the time until steady-state production is reached and the silver structure has reformed [6]. The changes can be both thermally or reaction induced, where the former result in a decrease in surface free energy. Morphological changes occurring as a result of reactions, between reactants or interactions with the catalyst, produce a structure different then what would occur in an inert atmosphere.

Oxygen is believed to induce a facet formation in silver to form thermodynamic favourable step or kink sites both by surface absorbed oxygen (O_α) and oxygen incorporated in the bulk (O_β). This result in a steady-state morphology for the silver in the formaldehyde syntheses as an equilibrium between thermal and oxygen induced influences [12].

Another observed morphological change in the silver surface from formaldehyde synthesis is the formation of so-called pinhole defects [6, 14]. Millar et al. preformed in-situ observations of pinhole formation at reaction temperatures above 600 °C. The holes were found in areas with surface defects, such as edges, and are believed to be the result of near-surface explosions created by sub-surface hydroxy recombination [14]. Waterhouse et al. suggest the hole formation may be due to the hydrostatic pressure created in the reaction between bulk-dissolved oxygen and hydrogen [6].

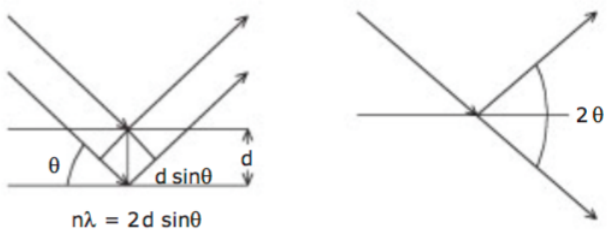

Figure 2.6: An illustration showing X-ray reflection related to Bragg's law in Equation 2.10. The figure is obtained from [18].

2.3 Catalyst Characterisation

Characterization of a catalyst involves the use of a series of techniques to identify physical, chemical and mechanical properties. It is an important part with the goal to gain a better understanding of how the catalyst work and how it can be improved and tailored to a specific need [18].

2.3.1 X-Ray Diffraction

X-ray diffraction (XRD) is a structural analysis technique and is often used to identify crystalline phases in the bulk and particle size in a crystalline material. Emitted X-ray photons are scattered by atoms in the sample and a diffraction pattern is created by the scattering which, due to the lattice sample parameters are unique for a particular compound. Diffraction patterns and lattice spacing are related by Bragg's law in Equation 2.10 [18],

$$n\lambda = 2dsin\theta; \quad n = 1, 2, ... \tag{2.10}$$

where n is an integer, λ is the X-ray wavelength, d is the distance between two lattice planes and θ is the angle between emitted and reflected X-ray radiation normal to the reflecting plane, as shown in Figure 2.6.

The technique have some drawbacks such as the XRD pattern is effected by the crystal size and amount of crystalline phase present in the sample and particles that are too small or amorphous can not be detected. Some of the limitations of the method present it self as a change in peak shape and intensity, but this information can be used to estimate particle size via the Scherrer formula in Equation 2.11. This formula relates crystal size and peak width,

$$L = \frac{K\lambda}{\beta cos\theta} \tag{2.11}$$

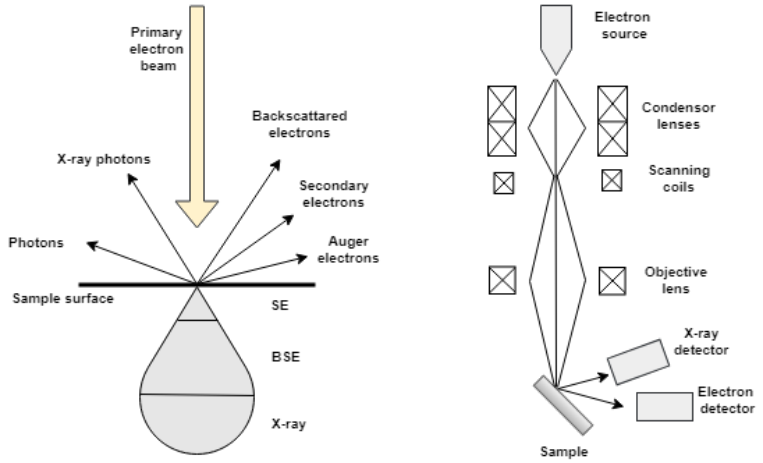

Figure 2.7: Left: Sketch showing the interactions between the primary electron beam and the sample in a electron microscopy setup. Right: Schematic set up of an scanning electron microscope with x-ray detector. The figure is inspired by [21].

where L is particle dimension, K is a constant, λ is the X-ray wavelength, β is the peak width (often at half peak height) and θ is the angle between emitted and reflected X-ray radiation normal to the reflecting plane [21].

2.3.2 Scanning Electron Microscopy

Electron microscopy is a frequently used technique investigating the field of surface science. It provides a way of inspecting the surface of a material by using electrons to create images with magnifications up till one million. A high energy electron beam is used and by studying the effect it exert on the sample a number of qualities can be investigated, such as illustrated to the left in Figure 2.7. The interactions can provide information related to morphology, crystallography and chemical composition of the material [21].

In a scanning electron microscope (SEM) the electron beam is focused by a set of lenses and scanning coils, to analyse a small part of the sample, which is set in a vacuum. Figure 2.7 (right side) shows a typical SEM set up. The energy level of the primary electron beam is usually in the range of 0.2 - 40.0 keV. Interactions between electron beam and the surface result in diagrams due to detection of backscattered electrons (BSE) or secondary electrons (SE) emission. In SEM the image contrast is a result of surface topography and sample composition. Backscattered electrons carry information about the heavy elements in a sample producing a contrast between elements. The secondary electrons are lower in energy then BSE, but give a better resolution. Surfaces facing the detector, and edges appear brighter then the surfaces facing away, crating a three dimensional effect [21].

Emitted X-ray radiation is characteristic for an element and can be used to identify chemical composition. This technique is called energy-dispersed x-ray analysis (EDX). To-

gether, these methods can create a good representation of a material surface.

SEM is a non destructive method and it can easily be used to investigate composition and changes in a catalyst surface. A disadvantage with SEM compared to other electron microscopy methods, is the low resolution (5 - 10 nm). Therefor, it is mainly used to characterise particles larger then 10 nm. Also, it may not provide a presentable image of a large surface, as only specific areas are scanned. The material must also be electron conducting, an issue that can be dealt with by coating the material, with, for example, carbon or gold [22].

2.4 Gas Chromatography

Chromatography is a frequently used analysis technique based on separation to identify molecular composition and quantities. It is based on the principle where samples will separate between two phases, one stationary and one mobile phase, due interactions between sample and the phases. The mobile phase is often a gas or liquid, defining the difference between gas and liquid chromatography. Several factors are important to achieve a successful separation of substances. Some of the conditions are the nature of the stationary and mobile phase, temperature and pressure [23].

A typical gas chromatograph (GC) set-up consists of several parts, where each has an important role. Figure 2.8 illustrate a typical set-up, highlighting the main parts. A carrier gas, the mobile phase, is often nitrogen, helium or hydrogen because it acts as an inert in the system and will transport the sample from the injection system trough the column to the detector. The sample is injected onto the column as a gas. When the sample and mobile phase reach the column the separation begins. Components can be separated by properties as weight, boiling point, volatility and polarity depending on the packing material, stationary phase, in the column. Last, the elements are detected and creates a signal based on mass or concentration. The signal made from detection is transformed to crate peaks in a chromatogram. Further result processing can be done on a computer [23]. An ideal detection system should result in sharp, symmetric, base separated peaks. The following section will explain more about the column and detector system.

Column

A solute migrating trough a column will, depending on its properties, interact with the stationary phase and absorb temporarily onto the liquid surface. This absorption cause the elements to travel through the column with a different velocity then the carrier gas. As a goal, the columns are tailored to be highly efficient, resulting in successfully separating solutes. Open-tubular capillary columns are the most common choice for GC analysis. The walls of the column can be coated with a film of liquid polymer (wall-coated open-tubular), where the side branches of the polymer are tailored to get suitable properties. Another option is coating the walls with a porous solid layer (porous-layer open-tubular) with a large surface area. Capillary columns often have a inner diameter of 0.2 - 0.7 mm and can be 10 - 100 m long. The capillary columns generally have a high efficiency due to the coating method and the column length, resulting in a high theoretical plate height,

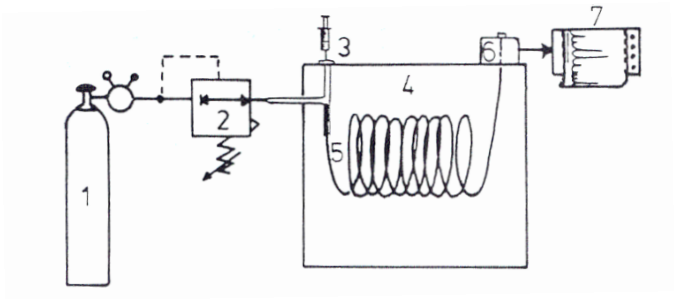

Figure 2.8: Illustration showing the general layout of an gas chromatograph. 1 = carrier gas, 2 = reduction valve, 3 = injector, 4 = oven, 5 = column, 6 = detector, 7 = result processing. The figure is obtained from [23].

a parameter for achieving efficient separation. It is important that the stationary phase is thermally stable and does not react with the samples [24, 25].

Detector

There are many different techniques to choose from when selecting a detection method. Flame ionisation, thermal conductivity detection and mass spectrometer are some of the frequent choices. The detection principle is either based on mass or concentration.

The thermal conductivity detector (TCD), which is used in this thesis experimental work, detects concentration levels. The concentration is proportional with the resulting signal and the method is therefor sensitive to varying flow rates. TCD is a universal, non-destructive detector and is mostly used for detection of organic and in-organic compounds, more specifically light and inert gasses.

As all compounds have the ability to absorb heat in some capacity, the detector is set up to measure the heat difference between two chambers. The carrier gas acts as a reference and flows through one heated chamber with a filament. An equilibrium will develop between the gas and the filament and this acts as a baseline against the second chamber. Here, gas exiting the column will flow trough. When a solute pass through the chamber some of the heat is absorbed and the difference in temperature can be detected as a change in current compared to the reference. This signal generate a peak in the chromatogram. Figure 2.9 show a sketch of a TCD system [24].

To achieve a sutible base line, carrier gas with a high thermal conductivity is used, as helium and hydrogen. A drawback with the system is the detectors low sensitivity, compared to other detectors, making it not ideal for detecting low concentrations. Eventually, the filaments burn out and need replacement. The lifetime is dependent on the system temperature and the corrosively and reactivity of the samples [23].

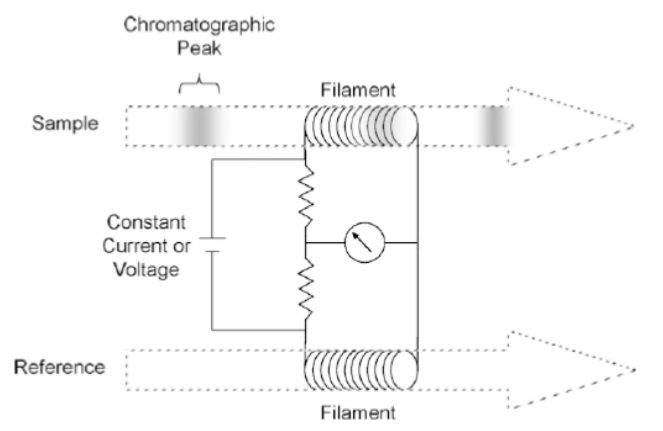

Figure 2.9: A sketch showing the working principle of a thermal conductivity detector used for gas chromatography. The figure is obtained from [24].

2.5 Catalytic Activity

Catalytic properties are measured to define catalyst performance. Activity measurements can be accomplished by measuring the reaction rate, conversion, selectivity, turnover frequency and stability. Some of the properties are specific to a set of process conditions and can not be generalised [18].

Turnover frequency (TOF) is a value that indicates the activity per active site on a catalyst. It is defined as number of molecules converted, or reacted, per active site, given in s^{-1}, as described in Equation 2.12. TOF is often a difficult catalyst property to specify as it is effected by the methods used for preparation, characterisation and it requires specific knowledge of the surface area under reaction conditions [26, 27].

$$TOF = \frac{Total\ number\ of\ reacted\ molecules}{Total\ number\ of\ sites \cdot time} \tag{2.12}$$

Conversion is also a term used to define activity. It is often used together with selectivity, as a fitting catalyst will produce the desired product. The definitions of conversion and selectivity are presented in Equations 2.13 and 2.14. Measuring conversion at a set space velocity or temperature for a fixed conversion are practical ways of measuring activity and is often used when catalyst comparisons are of interest [26].

$$Conversion = \frac{Amount\ of\ reagent\ consumed}{Amount\ supplied} \tag{2.13}$$

$$Selectivity = \frac{Moles\ of\ desired\ product\ formed}{Moles\ of\ desired\ product\ stoichiometrically\ possible} \tag{2.14}$$

In this study conversion, selectivity and stability are used to measure activity.

Chapter 3

Experimental

3.1 Health, Safety and Environment

Experimental work was performed at NTNU laboratories, in accordance with the existing rules and regulations regarding health, safety and environment (HSE), including working after normal work hours routines. The main risks associated with the work are using explosive and toxic gases at high temperature when operating the methanol to formaldehyde set-up. The risk is acceptable, as the set-up is enclosed with proper ventilation system, safety valves and controllers. Routines were followed to ensure a safe work environment, such as leak testing, using hydrogen and carbon monoxide detectors and correct protective gear. A risk assessment for the experimental work was prepared as a part of the requirements of the master thesis and is accessible in full, at the university risk assessment portal with ID-number 22597.

3.2 Catalyst Characterisation

3.2.1 X-Ray Diffraction

X-ray diffraction was performed using a diffractometer of the model D8 DaVinci Advanced with the software Diffrac.Measuerment Centre v6.5.0. The instrument use a Cu anode with Kα radiation, wavelength of 1.54Å. The samples were analysed using a method for crystalline samples measuring at 2θ angles from 35 to 105 degrees with fixed V6 slit. The fixed slit illuminates 6 mm of the sample at all angles. To ensure an homogeneous sample with a level surface, the silver particles were ground with a mortar and pestle before added to a sample holder (Si 10 mm cavity). Further result processing was performed using Diffrac.Eva v4.2.1.10 software for identifying metal phases and crystal size.

3.2.2 Scanning Electron Microscopy

Scanning electron microscope was used to analyse the silver samples after each experiment, in addition to fresh catalyst. The instrument used was of the model Hitachi S-3400N. A secondary electron detector was used to investigate the silver morphology. For this analysis an acceleration voltage of 15 keV, with 40 % probe current at about 5 mm working distance and the images were captured at a speed of 40 seconds. Silver samples were mounted on a sample holder using carbon tape.

EDX analysis was performed on specific samples using an X-ray detector. The acceleration voltage varied based on which element was of interest. For silver detection 7 keV and 15 keV were used and the probe current and working distance were increased to 50 % and 10 mm.

3.3 Catalyst Analysis

A series of experiments were performed to investigate catalytic activity and morphological changes. Polycrystalline silver particles (0.25 - 0.50 mm) were used for all experiments, produced by electrolysis at K.A. Rasmussen. To resemble industrial process conditions for formaldehyde production the temperature of 650 °C and interval between 200 to 700 °C were chosen for all experiments. Atmosphere and experiment length a varying parameter during the testing. An overview of the experiments and parameters are shown in Table 3.1.

Table 3.1: Variables and parameters used during the experiments on the Ag catalyst.

Atmosphere	**TOS [hours]**	**Temperature [°C]**	**Activity**
Nitrogen	5^{α}, 24	650	-
Air	5^{α}, 24^{α}, 72	650	-
Hydrogen	5^{α}, 24^{α}	650	-
Methanol/Water	24	650	-
H_2 oxidation	-	200 - 700	Yes
CO oxidation	-	200 - 700	Yes
Methanol oxidation	-	200 - 600	Yes

$^{\alpha}$ Performed during the Specialization Project

Experiments without catalyst were also performed to investigate gas phase activity. All experiments were performed in a calcination oven set-up and in the methanol to formaldehyde (MTF) test set-up, to be presented in the following sections.

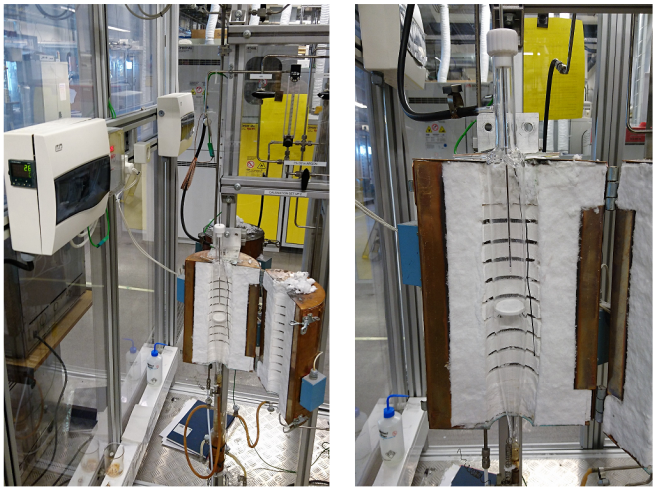

Figure 3.1: Image of the calcination set-up showing the eurotherm, valve system and oven with reactor to the left and a close-up of the oven with the reactor to the right.

3.3.1 Experimental set-up

Calcination set-up

The calcination set-up consists of gas cylinders, where the gas is feed through stainless steel pipe lines with Swagelock fittings, to a glass reactor placed in an isolated oven. The gas flow is regulated using a rotameter (0 - 120 ml/min) and is ventilated via a water seal. A N-type thermocouple and Eurotherm were used to measure and regulate the oven temperature and can be used to set a temperature program fit for the experiment. The set-up is shown in Figure 3.1.

Methanol to formaldehyde test set-up

The methanol to formaldehyde (MTF) experimental set-up is mainly used to perform catalytic activity testing related to the industrial MTF process. A process flow diagram for the MTF set-up is presented in Figure 3.2.

The main components in the set-up consist a set of pressure regulators, mass flow controllers (MFC), liquid tanks, vaporizer and a reactor, set in an isolated oven. Gas is feed through four high pressure stainless steel pipe lines (1/4”), with Swagelock fittings. Two lines are used for nitrogen, at different volumetric flow rates (4 - 200 Nml/min and 30 - 1500 Nml/min), one line is used for synthetic air (10 - 500 Nml/min) and the last is for CO or H_2 gas (1 - 100 Nml/min). Two stainless steel containers are used to hold methanol/water and formaldehyde solution and are pressurised with helium gas. All the pipe lines are equipped with pressure regulators and valves used for manual control. The system is operated at ambient pressure and one mechanical safety valve is placed before the reactor to prevent pressure build up. Gas and liquid are introduced to the system by

the mass and liquid flow controllers (Bronkhorst), which is digitally controlled by the software, LabVIEW v.13. An evaporator (CEM - Controlled Evaporation and Mixing) is used to mix and vaporise the feed before entering the fixed bed reactor, which is made of quartz glass. Details regarding the reactor design is shown in Appendix A, Figure A.2. A bypass line is also available to avoid the CEM and reactor.

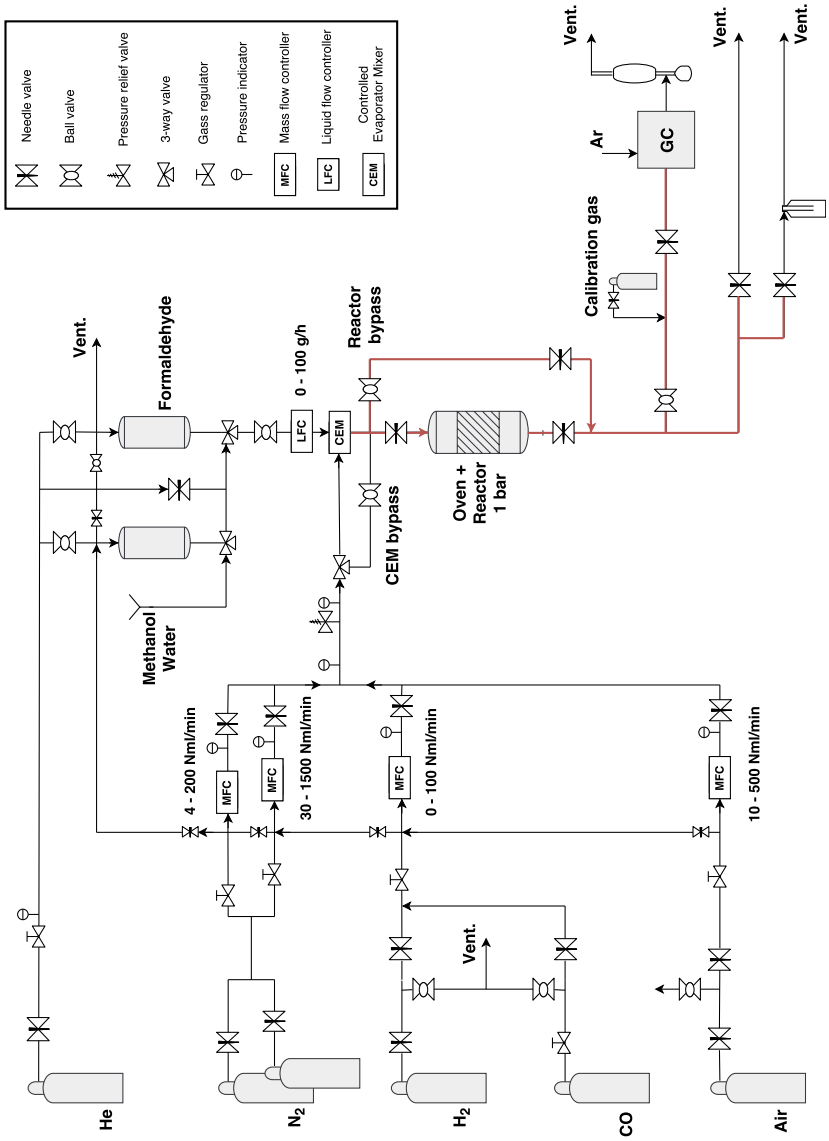

Figure 3.2: Process flow diagram of the MTF test set-up per January 2018.

A gas chromatograph is used to analyse the product and feed stream (Agilent Technologies 7890A) and is operated by the program GC ChemStation. An automatic valve system, which is operated by pressurised air, control the sample injection. The GC uses two columns, molsieve 5A and CP-sil 5 CB columns, to separate the product gas and use thermal conductive detectors (TCD) for detection. The PLOT molsieve column is used to detect light weigh gases, such as hydrogen, oxygen, methane, nitrogen and carbon monoxide. The WCOT CP-sil column separate compounds based on boiling point and is used for methane, carbon dioxide, methanol, formaldehyde, formic acid and water separation. An illustration of the automated injection valve system is shown in Appendix A, Figure A.1.

Pipelines from the evaporator to the GC are heated by electric heating bands and isolated to prevent condensation and thermocouples (K-type) are used to monitor the temperature with the software EasyVIEW. One thermocouple is placed inside the reactor and is used to measure the temperature profile in the reactor by moving the thermocouple vertically.

Prior to the experiment leak tests are performed with nitrogen and leak test spray, followed by hydrogen or carbon monoxide (2 mol%) and using a gas detector.

Mass and liquid flow controllers, in addition to the GC, were calibrated during the specialization project and master thesis project period.

Calibration

Mass flow controllers were calibrated using a bobble flow column, where a flow was set in LabVIEW and the bubble travel time was measured corresponding to a fixed column volume. The liquid flow controller was calibrated by weighing samples of methanol/water and pure methanol produced by the controller for a set time period. Further, the GC was calibrated by analysing calibration gas with compositions shown in Table 3.2. Parameters, retention time, concentration and area, were adjusted based on the calibration gas analyses. The GC was also calibrated for formaldehyde, by manual injection of a standard solution (27.6 mol%).

Calibration curves for the flow controllers are shown in Appendix A, Figures A.3 to A.10.

Table 3.2: Composition of the calibration gases used to calibrate the GC.

Component	Concentration [mol%]
Hydrogen	5
Methane	1
Carbon dioxide	1.5
Carbon monoxide	0.5
Nitrogen	Balance
Methanol	0.5
Nitrogen	Balance

3.3.2 Calcination Experiments

Calcination experiments were performed to investigate the effect of varying atmospheres had on the silver morphology.

Experiments with nitrogen (5.0) and air (synthetic) were performed in the calcination set-up. Silver catalyst was added to a calcination reactor ($\sim$ 1 g), using a quartz sinter as support, and installed in an isolated oven. A gas line was connected to and from the reactor and flow was set using a rotameter. The total flow for the experiments were set to 100 ml/min. An Eurotherm was programmed to hold the oven temperature at 650 °C at a given time period and set the heating and cooling rate at 10 °C/min.

Experiments performed with H_2 (1 %) in nitrogen and a mix of methanol (8 mol%) and water (H_2O/CH_3OH:1.34), were carried out in the MTF set-up. The feed compositions are shown in Table 3.3. The temperature program is similar as for the previously mentioned experiments, but increased to 700 °C to compensate for heat loss. Total flow for the experiments were set to 250 Nml/min. The reactor was assembled with a silver bed containing a quartz sinter, a layer of quartz wool as support and silver particles, as shown in Figure 3.3.

Table 3.3: Flow set points for hydrogen (top) and methanol/water (bottom) calcination experiments. The total flow was set to 250 Nml/min.

Component	**Flow [Nml/min]**
Hydrogen	2.5
Nitrogen	247.5
Methanol	20
Water	23.6
Nitrogen	206.4

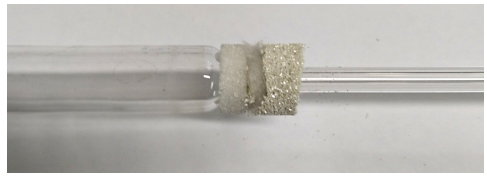

Figure 3.3: Catalyst bed for calcination experiments in the MTF test set-up. From the left; quartz sinter, quartz wool and silver particles.

3.3.3 Oxidation Experiments

Oxidation experiments were performed with hydrogen, carbon monoxide and methanol to investigate catalytic activity and how reactions influence the silver morphology. Experiments were performed with both a heating and cooling sequence, between 200 and 700 °C

with a 45 minute hold at every 100 °C, as shown in Figure 3.4. The temperature profile trough the reactor was measured at every 100 °C. An Eurotherm was used to set the temperature program which was programmed using the software iTools Engineering Studio. Product gas was continuously analysed by the GC.

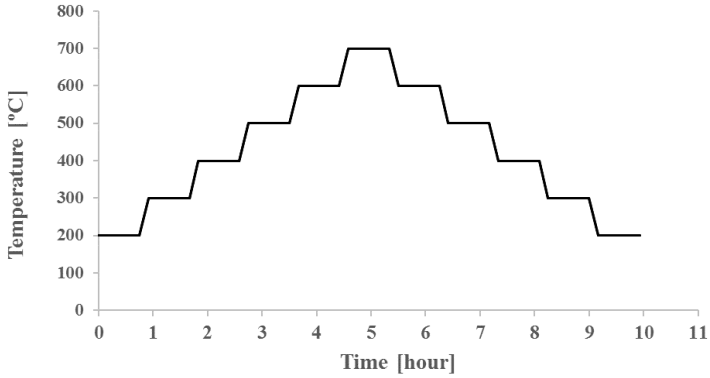

Figure 3.4: Graph showing the temperature program used in oxidation experiments in the MTF set-up.

Blank experiments, without catalyst, were performed to investigate gas phase reactions and confirm the effect of the catalyst for H_2 and CO experiments. The catalyst bed was of identical design as described in Figure 3.3. For experiments using the same catalyst bed the reactor was flushed with nitrogen between runs.

Previous to the experiments a feed analysis was performed by GC analyses to be used in calculations. GC analyses were continued until stable values were achieved.

Hydrogen and Carbon Monoxide Oxidation

Hydrogen and carbon monoxide oxidation experiments were performed at conditions shown in Table 3.4. Experiments were performed with catalyst ($\sim$ 250 mg), H_2 or CO (2 mol%), in excess oxygen (6 mol%), which was supplied as air. Two different silver beds were used to investigate the reproducibility of the experiment (referred to as catalyst bed 1 and 2), in addition to see if the prolonged used of the silver effected the morphology. The catalytic activity was also tested over time, for three days, followed by a cooling sequence. In Table 3.5 the flow set points are shown. Oxidation experiments were performed equally with two exceptions, both occurred during the hydrogen oxidation experiments. The experiment using catalyst bed 1 were performed 1 mol% H_2 and a temperature program with 30 minute hold each 50 °C. The experiment using catalyst bed 2, experiment 2 were performed with a temperature program with 30 min hold each 100 °C.

Methanol Oxidation

Only one methanol oxidation experiment with catalyst was performed due to equipment malfunction. The experiment was performed with a similar temperature program as described in Figure 3.4. About 450 mg catalyst was used with 8 % methanol and a methanol

Table 3.4: H_2 and CO oxidation experimental overview showing the temperature range, time on stream and which catalyst bed was used.

Experiment	Catalyst bed	Temperature [°C]	TOS [hours]
H_2/CO oxidation	Blank	200 - 700	6
	Catalyst bed 1.1*	200 - 700 - 200	12
	Catalyst bed 2.1	200 - 700 - 200	12
	Catalyst bed 2.2°	200 - 700 - 200	12
	Catalyst bed 2.3	700 - 200	72

*Performed with 1 mol% H_2 30 min hold each 50 °C for H_2 ox.

°Performed with 30 min hold each 100 °C for H_2 ox.

Table 3.5: Flow set points for H_2 and CO oxidation experiments performed in the MTF set-up. Experiments were performed with 2 % H_2, O_2/H_2:3 ratio and a total flow of 250 Nml/min.

Component	Flow [Nml/min]	Concentration [mol%]
Nitrogen	230.0	92.0
O_2	15.0	6.0
H_2/CO	5.0	2.0

to oxygen ration of 2.314, as provided by Dynea AS. Oxygen was supplied as air. In Table 3.6 the flow set points are shown. The experiment produced activity data until 700 °C was reached. For this type of experiment H_2O is usually a part of the reactant stream. In this case, it was of interest to investigate if, and what effect was shown when H_2O was removed from the feed, in addition to activity data.

3.3.4 Calculations

From the continuous GC analyses the information could be further analysed using Microsoft Excel. Conversion, defined as converted reactant, was calculated for the relevant experiments. Nitrogen is an inert in the reaction system and was used as an internal standard in the calculations. To validate the calculations a mass balance over the system can

Table 3.6: Flow set points for methanol oxidation experiment performed in the MTF set-up. Experiments were performed with 8 mol% methanol, MeOH/O_2:2.314 ratio and a total flow of 500 Nml/min.

Component	Flow [Nml/min]	Concentration [mol%]
Nitrogen	442.7	88.5
O_2	17.3	3.5
Methanol	40.0	8.0

be performed [28]. Examples on the calculations are shown in Appendix C.

Conversion

Conversion of a reactant can be calculated by Equation 3.1. The flow of any reactant can be defined by Equation 3.2, where F_{TOT} is the total flow and y_i is the component mole fraction, provided by the GC analysis for a given component, i. y_i is generated by the components thermal conductivity, transformed via an electric signal to a peak in the chromatogram, with a specific area and response time.

$$\mathrm{X_{reactant}} = \frac{\mathrm{F_{reactant,in}} - \mathrm{F_{reactant,out}}}{\mathrm{F_{reactant,in}}} \tag{3.1}$$

$$\mathrm{F_{reactant}} = \mathrm{y_i} \cdot \mathrm{F_{Tot}} \tag{3.2}$$

Further, the reactant H_2 is used as an example. Combining Equations 3.1 and 3.2, the conversion of hydrogen can be expressed by Equation 3.3.

$$\mathrm{X_{H_2}} = \frac{\mathrm{y_{H_2,in}F_{Tot,in}} - \mathrm{y_{H_2,out}F_{Tot,out}}}{\mathrm{y_{H_2,in}F_{Tot,in}}} \tag{3.3}$$

Next, with the assumption that all converted reactant produce the desired product and the total flow into the system is not assumed to be equal to the total flow out of the system, the total flow can be expressed using the inert, N_2. Finally, by combining Equations 3.3 to 3.5, the conversion can be expressed by Equation 3.6.

$$\mathrm{F_{Tot,in}} = \frac{\mathrm{F_{N_2,in}}}{\mathrm{y_{N_2,in}}} \tag{3.4}$$

$$\mathrm{F_{Tot,out}} = \frac{\mathrm{F_{N_2,out}}}{\mathrm{y_{N_2,out}}} \tag{3.5}$$

$$\mathrm{X_{H_2}} = 1 - \frac{\mathrm{y_{H_2,out}}}{\mathrm{y_{H_2,in}}} \frac{\mathrm{y_{N_2,in}}}{\mathrm{y_{N_2,out}}} \tag{3.6}$$

Conversion can also be calculated by the amount of reacted oxygen or by the amount of formed product.

Selectivity

As a measurement on how much desired product is produced based on consumed reactant in the reaction selectivity is used. In this case, the carbon selectivity can be calculated as a function of the total amount of converted methanol or as a function of the total amount of produced carbon products. Selectivity can also be calculated based on hydrogen, but is not done in the thesis due to the instability of water GC analys.

Equation C.3 show how to calculate the selectivity of CH_2O based on the total amount of converted methanol. The carbon product method is shown in Equation 3.8 for component, i.

$$S_{CH_2O} = \frac{F_{Tot,out} y_{CH_2O,out}}{F_{Tot,in} y_{CH_3OH,in} - F_{Tot,out} y_{CH_3OH,out}} \tag{3.7}$$

$$S_{C,i} = \frac{y_{C,i,out}}{\sum y_{C,product,out}} \tag{3.8}$$

In this thesis Equation C.3 is used, due to uncertainty of the specific amount of carbon products.

Mass balance

A mass balance over the system is calculated as a validation of the experimental set-up and methods of detection. In general, an error with the limit of 5 % is accepted due to systematic errors like gas leakages and simplifications.

As an example, by assuming all hydrogen either reacts to form water or leave the system as un-reacted hydrogen the following component balance can be expressed in Equation 3.9.

$$F_{H_2,in} = F_{H_2,out} + F_{H_2O,out} \tag{3.9}$$

When applying the correlations in Equations 3.1 and 3.2, the error in the hydrogen balance can be calculated by Equation 3.10,

$$E_H = \frac{F_{Tot,out} \sum n y_{H,out} - F_{Tot,in} \sum n y_{H,in}}{F_{Tot,in} \sum n y_{H,in}} \tag{3.10}$$

where, n, is a stoichiometric factor. The same balance can be carried out for the components, oxygen and carbon.

Chapter 4

Results

4.1 Catalyst Characterisation

4.1.1 X-Ray Diffraction

The X-Ray diffractrograms for the silver samples exposed to various atmospheres are presented in Figure 4.1, where Fresh Ag is indicated by black, N_2 calcination (24 hours) by red, MeOH/H_2O calcination by blue, H_2 oxidation by green and CO oxidation by brown. The intensity of the different phases are indicated by peak height. The crystalline face-centred cubic silver and the phases were identified by comparison in the Diffrac.Eva software database. The peaks exhibit similar characteristics and no great change is evident. In the diffractogram representing N_2 calcination, the (200) and (220) phases have increased intensities compared to the fresh Ag. Peaks representing the (111) and (311) phases in the silver used for CO oxidation also have increased in intensities.

Crystallite size for the samples were calculated using the Scherrer formula (see Chapter 2.3.1) in the Diffrac.Eva software, with a K-value of 0.89 and using full width at half maximim (FWHM). The values are presented in Table 4.1 and the crystallite size has not been effected noticeably by the various experimental treatment. Catalyst used in oxidation experiments show a slight decrease in size compared to the fresh silver catalyst.

4.1.2 Scanning Electron Microscopy

Experiments using silver catalyst, as listed in Chapter 3, Table 3.1, were performed to investigate if the catalyst morphology was effected when exposed to various atmospheres at industrially relevant temperatures and conditions. Scanning electron microscope (Hitachi S-3400N) was used to analyse the silver and the scans will be presented in the following

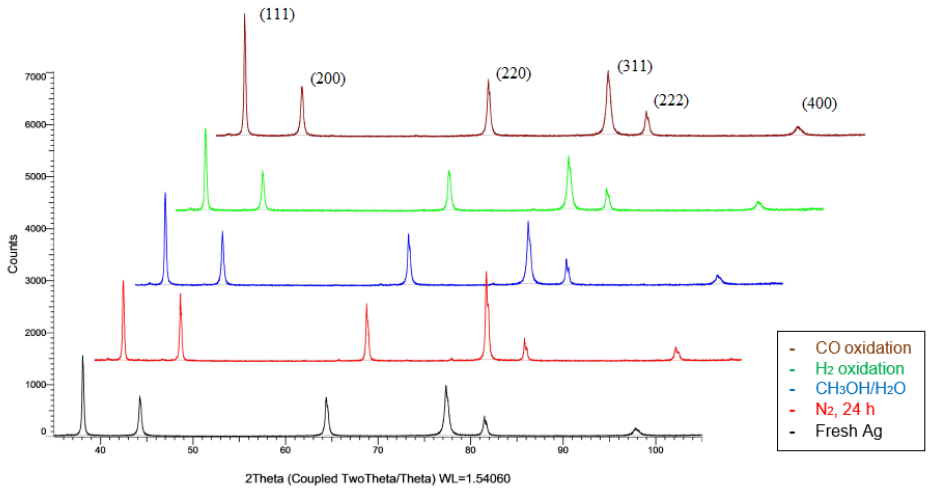

Figure 4.1: X-Ray Diffraction pattern for the silver catalyst exposed to various conditions. Black = Fresh Ag, Red = N_2 calcination (24h), Blue = CH_3OH/H_2O, Green = H_2 oxidation, Brown = CO oxidation

Table 4.1: Calculated crystallite size for a set of silver samples exposed to various atmospheres, using the software Diffrac.Eva, K-value = 0.89 and FWHM.

Experiment	**Crystallite size [nm]**
Fresh Ag	37.5
N_2, 24h	37.9
CH_3OH/H_2O	37.9
H_2 oxidation	33.1
CO oxidation	34.9

section. Image editing tools have been used to adjust, such as brightness and contrast, to improve the image quality. Unfortunately, this will not guarantee for sufficient image quality in print.

Fresh Silver Catalyst

A sample of unused silver catalyst was analysed to be used as a referance for comparison. Figure 4.2 show the silver at two different magnifications. At low magnification, (a), a clear faceted structure is visible and at higher magnifications, (b), a terrace structure and surface defects in the metal are shown. The silver is produced by electrolytic refining, promoting a structure with a large surface area.

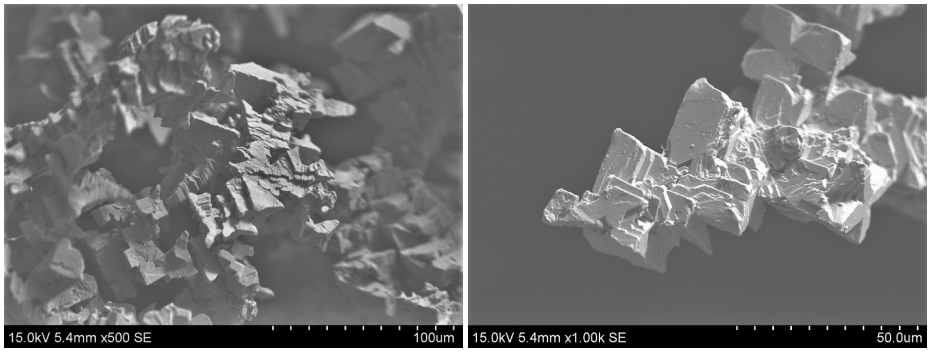

(a) **(b)**

Figure 4.2: SEM images of unused particular silver catalyst at different magnifications ((a): x500, (b): x1.00k) using secondary electron detector.

Nitrogen Atmosphere

The silver was exposed to nitrogen at 650 °C for 5 and 24 hours in the calcination set-up. From the images in Figure 4.3, structural changes in the silver are evident. In the high magnification images, (b), the terrace structures are less pronounced, but still visible. Widespread holes are also visible in the structures, but are not consistent throughout the sample. The experiment length does not seem to significantly influence the hole size or silver morphology.

Hydrogen Atmosphere

Figure 4.4 show SEM images from hydrogen (1 mol%) calcination in the MTF set-up, for 5 and 24 hours with temperature set point at 650 °C. Due to a heat gradient in the set-up the actual temperature in the catalyst bed was 600 °C. Compared to the unused catalyst sample, facet and terrace structures seem to be intensified in the hydrogen atmosphere and minor hole formations are present. Lengthened exposure time does not seem to have a great impact on the silver morphology.

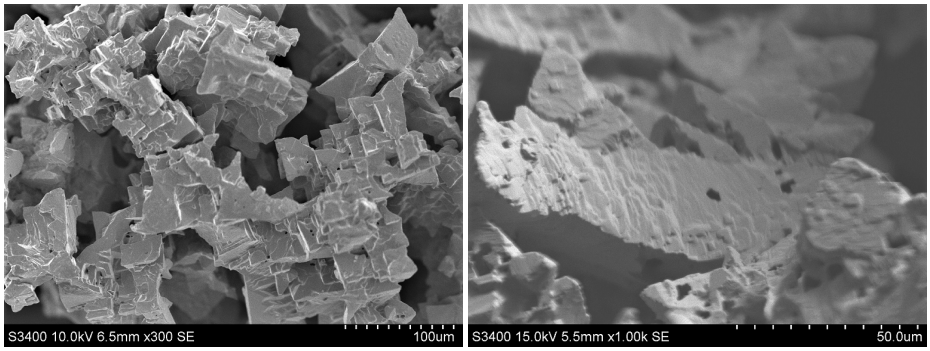

(a) **(b)**

Figure 4.3: SEM images of silver catalyst exposed to nitrogen for 5 and 24 hours, at different magnifications ((a): 5h, x300, (b): 24h, x1.00k) using secondary electron detector.

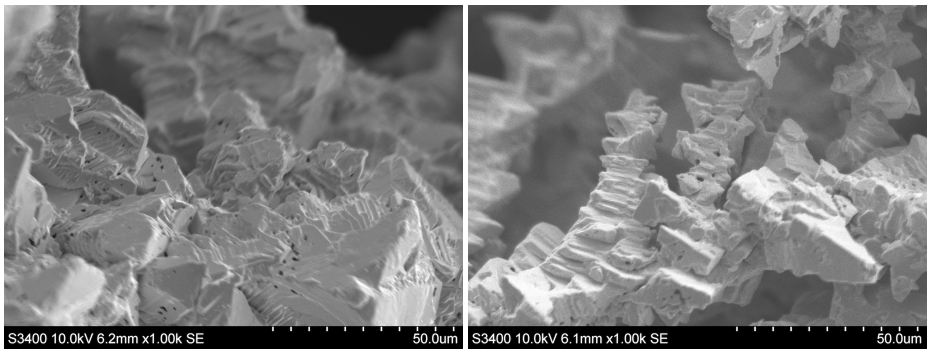

(a) **(b)**

Figure 4.4: SEM images of silver catalyst exposed to hydrogen (1 mol%) for 5 and 24 hours, at similar magnifications ((a): 5h, x1.00k, (b): 24h, x1.00k) using secondary electron detector.

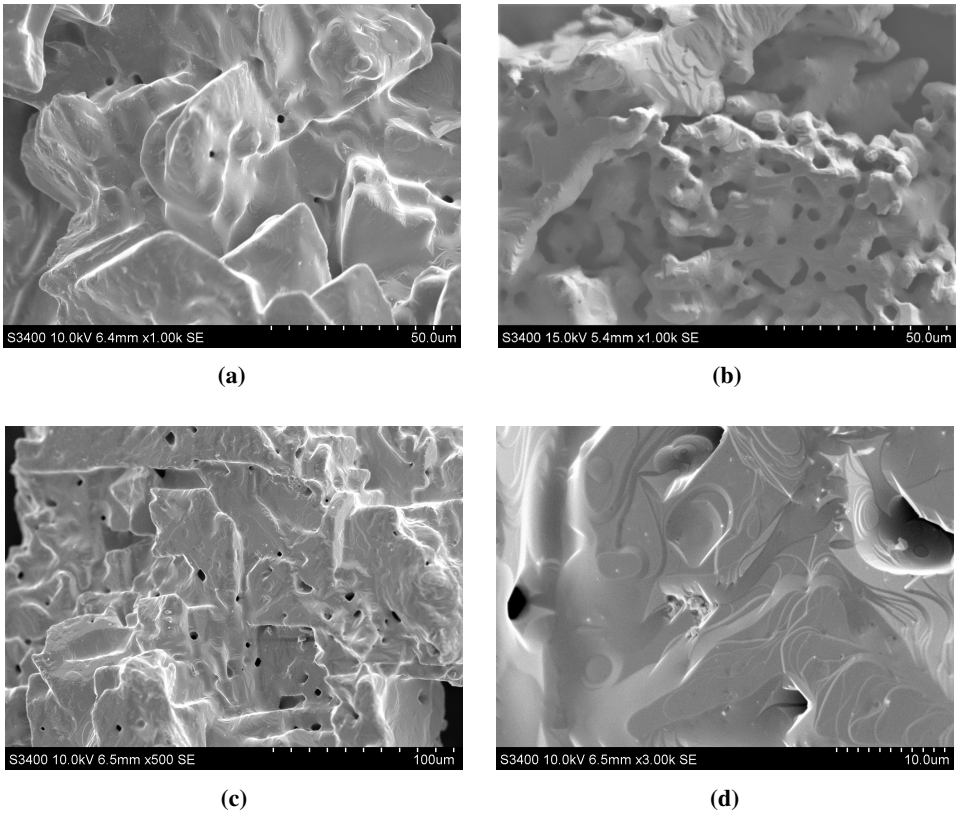

(a) **(b)**

(c) **(d)**

Figure 4.5: SEM images of silver catalyst exposed to air for 5, 24 and 72 hours, at various magnifications ((a): 5h, x1.00k, (b): 72h, x1.00k, (c): 24h, x500k, (d): 24h, x3.00k) using secondary electron detector.

Air Atmosphere

The silver was exposed to synthetic air at 650 °C for 5, 24 and 72 hours in the calcination set-up. From the images in Figure 4.5 great changes in topology for all samples are evident. The morphological changes are more extensive as the exposure time increase, resulting in larger and an increased number of holes at 72 hours (Figure 4.5 (b)). The angular grain structure is eliminated and at higher magnification (Figure 4.5 (d)) well-defined facets are visible. The facet structure and hole formation has only been clearly visible in calcination experiments where oxygen has been present.

Methanol and Water Atmosphere

The silver was exposed to a CH_3OH/H_2O atmosphere for 24 hours at 650 °C in the MTF set-up. From the images in Figure 4.6 no great structural changes in the silver are evident as similar to the fresh silver and nitrogen calcination experiment. During the experiment GC analysis was performed and trace amounts of CH_2O and H_2 were detected.

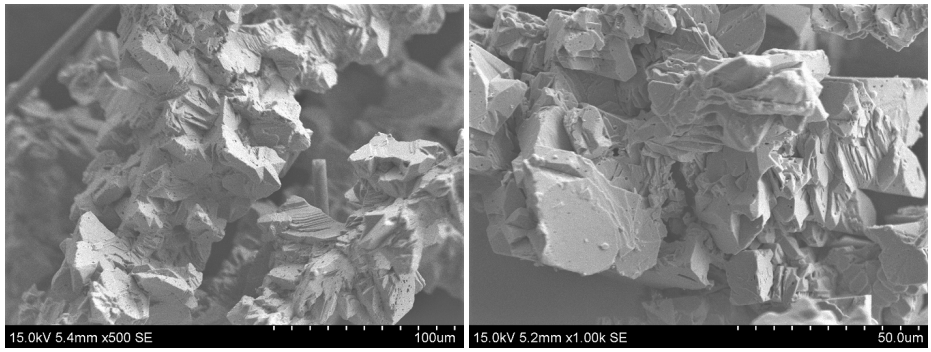

(a) **(b)**

Figure 4.6: SEM images of silver catalyst exposed to a methanol and water vapour atmosphere for 24 hours, at different magnifications ((a): x500, (b): x1.00k) using secondary electron detector.

Hydrogen Oxidation

Silver particles were used as a catalyst in hydrogen oxidation experiments producing water. Two catalyst beds were used, one for a single experiment, noted as ”Catalyst bed 1”, where the temperature was increased step-wise to set point temperature of 700 °C and cooled back to room temperature. This experiment was performed over the course of two days, and the reactor was exposed to a nitrogen atmosphere over night at high temperature. The second bed, ”Catalyst bed 2”, was used in two heating/cooling experiments, in addition to a three day period at set point temperature of 700 °C. Between the experiments the reactor was exposed to a nitrogen atmosphere over a longer period of time.

In Figure 4.7 the SEM images for both the silver catalyst beds are shown and great changes in topology for all samples are evident. The angular grain structure is eliminated and at higher magnification (Figure 4.7 (d)) well-defined facets are visible, particularly in Catalyst bed 2. Images of Catalyst bed 1 show more frequent and larges holes then Catalyst bed 2, where the structure is smoother and holes are smaller.

Carbon Monoxide Oxidation

Silver particles were used as a catalyst in oxidation of carbon monoxide experiments producing carbon dioxide. Two catalyst beds were used, one for a single experiment, described as ”Catalyst bed 1”, where the temperature was increased step-wise to set point temperature of 700 °C and cooled back to room temperature. During the experiment the laboratory experienced a power shortage, lasting about 45 min. For that time the temperature slowly declined in the reactor and oven, but was increased back to correct temperature when the power returned. The temperature was keep stable for one hour before continuing the temperature program. The second bed, ”Catalyst bed 2”, was used in two heating/cooling experiments, in addition to a three day period at set point temperature of 700 °C. Between the experiments the reactor was exposed to a nitrogen atmosphere over a longer period of time.

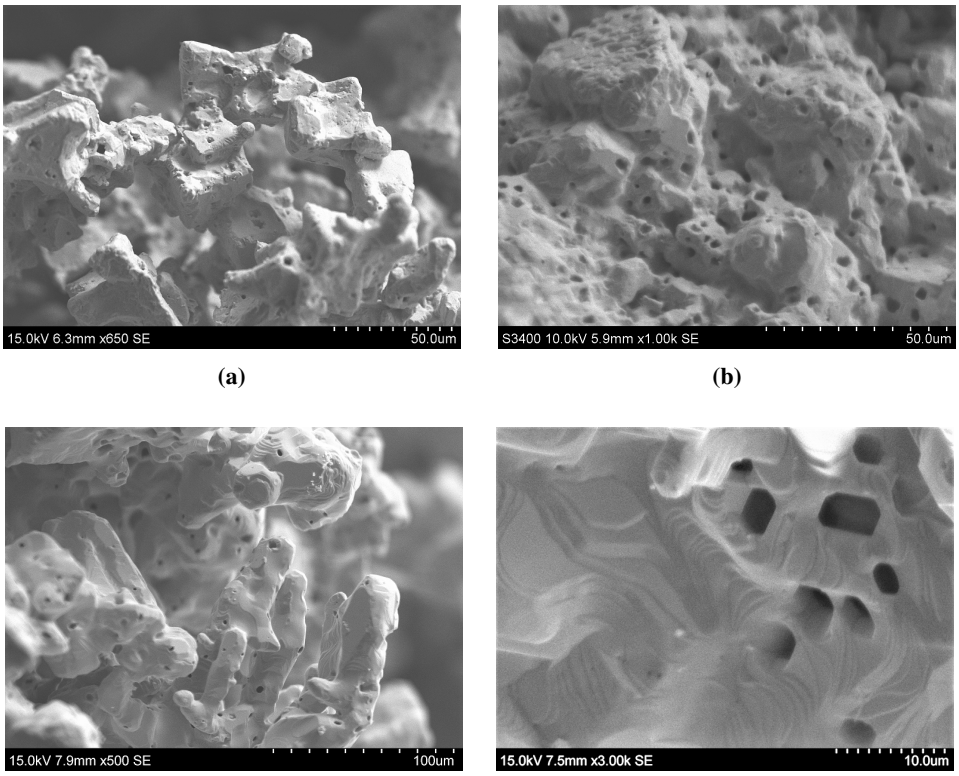

(a) **(b)**

(c) **(d)**

Figure 4.7: SEM images of silver catalyst used in hydrogen oxidation experiments, at various magnifications ((a): Catalyst bed 1, x650, (b): Catalyst bed 1, x1.00k, (c): Catalyst bed 2, x500k, (d): Catalyst bed 2, x3.00k) using secondary electron detector.

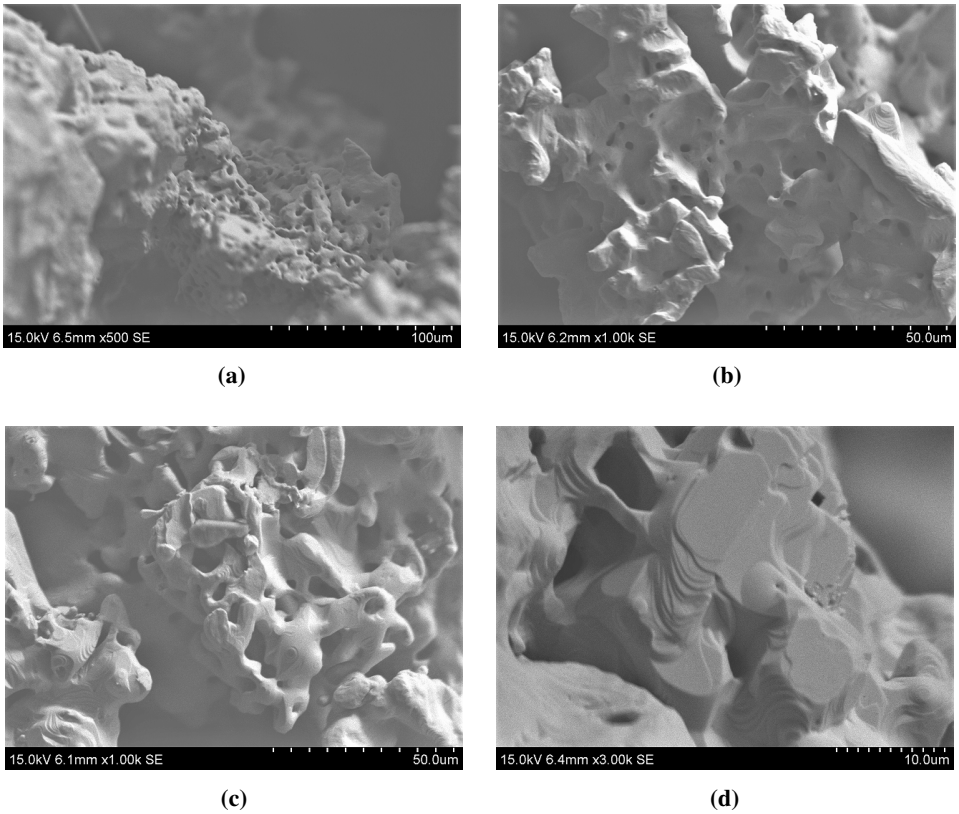

Figure 4.8: SEM images of silver catalyst used in carbon monoxide oxidation experiments, at various magnifications ((a): Catalyst bed 1, x500, (b): Catalyst bed 1, x1.00k, (c): Catalyst bed 2, x1.00k, (d): Catalyst bed 2, x3.00k) using secondary electron detector.

In Figure 4.8 the SEM images for both the silver catalyst beds are shown and great changes in topology for all samples are evident. The angular grain structure is eliminated and at higher magnification (Figure 4.8 (c) and (d)) well-defined facets are visible, particularly in Catalyst bed 2. A greater degree of smoothing also seem to be evident in Catalyst bed 2.

Methanol Oxidation

Silver particles were used as a catalyst in a oxidation of methanol experiment. Experimental equipment broke down half way into the experiment, resulting in only 5 hours on stream for the catalyst and being the only methanol oxidation experiment performed. The catalyst bed was analysed by SEM and the result is shown in Figure 4.9. Dark spots were noticed visually on top of the catalyst bed after use (Figure 4.10 (right)) and both bulk and top of the catalyst bed were analysed. This was further investigated by EDX analysis.

In Figure 4.9 different morphologies are shown. Bulk analysis does not revile a great structural change, as shown in, a, to the left. Clear terrace structure is present, similar as

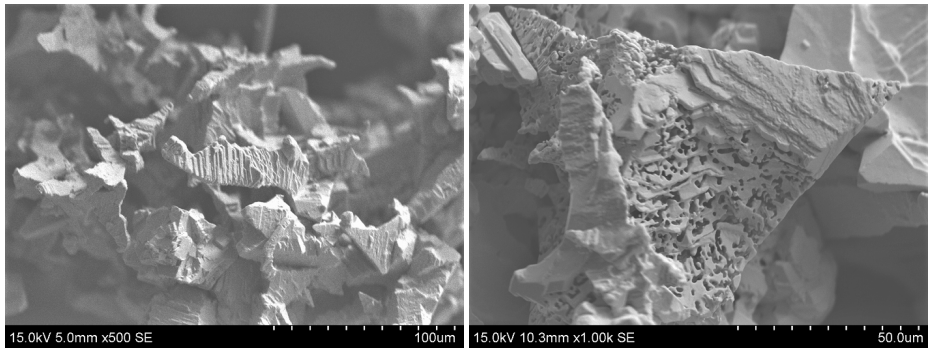

(a) **(b)**

Figure 4.9: SEM images of silver catalyst used in methanol oxidation experiment, at different magnifications ((a): x500, (b): x1.00k) using secondary electron detector.

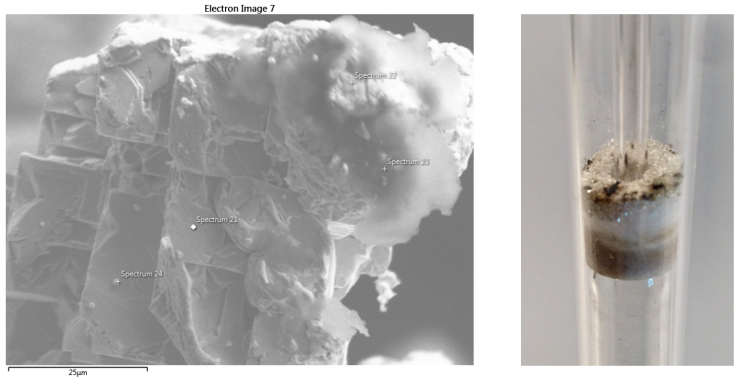

Figure 4.10: Left: SEM image from EDX analysis, of silver catalyst used in methanol oxidation experiment at x1.50k magnification using X-ray detection. Right: Image of the catalyst bed used for methanol oxidation after ended experiment, showing dark spot on the top of the bed.

to fresh catalyst in Figure 4.2. Analysis of silver from the top of the bed clearly shows a large number of holes produced on the surface.

EDX analysis was performed on silver from the top of the catalyst bed. Figure 4.10 (left) show the scan used for the analysis and marks the locations of the EDX analysis. The silver show no noticeable structural changes. Table 4.2 present the EDX results and the elements detected on the surface of the silver particle. In the ”cloud-like” formation to the right in the image, silver, carbon and oxygen are the elements detected. Silicon is also detected, but only as trace amounts.

Table 4.2: EDX analysis of silver catalyst used in methanol oxidation experiment. The spectrum relate to a position in Figure 4.10.

Spectrum 21	**Wt%**	**Spectrum 22**	**Wt%**
Ag	100	Ag	90.8
		C	9.2
Spectrum 23		**Spectrum 24**	
Ag	52.0	Ag	100
C	46.0		
O	2.0		
Si	0.1		

4.2 Catalyst Activity

Catalyst activity experiments were performed as described in Section 3.3.3. In the following section results from the analysis will be presented.

Each experimental run produced flow and temperature logs, chromatograms from the GC and temperature measurements from the thermocouple placed in the reactor. Experimental data was compared based on the logged time stamps to correlate temperatures and GC data. Also, to ensure correct and stable temperature for the data points. The GC chromatograms provided data used to calculate conversion and selectivity of hydrogen, carbon monoxide and methanol in the respective oxidation experiments. All calculations are based on Equations 3.6, C.3 and 3.10, presented in Section 3.3.4 and calculation examples are presented in Appendix C.

Temperature logs and temperature profiles over the catalyst bed, were used to match average conversion data and stable reactor temperature, every 100 °C between 200 °C and 700 °C, for both reactor heating and cooling sequences. The conversion was then plotted against the appropriate catalyst bed temperature.

For each experiment the accuracy was calculated by a mass balance over the reaction. This was done by using the mass balance Equation 3.10, in Section 3.3.4 and GC data.

Typical feed analysis for the various experiments are shown in Appendix B, Tables B.1 to B.3.

4.2.1 Hydrogen oxidation

Hydrogen oxidation experiments were performed in the MTF set-up to investigate the catalytic activity of silver for the reaction presented in Section 2.1, Equation 2.8. The experiments were performed with polycrystalline silver catalyst, in addition to one reference test without catalyst. For experiments with catalyst the reactor was set up as shown in Section 3.3, Figure 3.3. Temperature profiles over the catalyst bed were measured for each

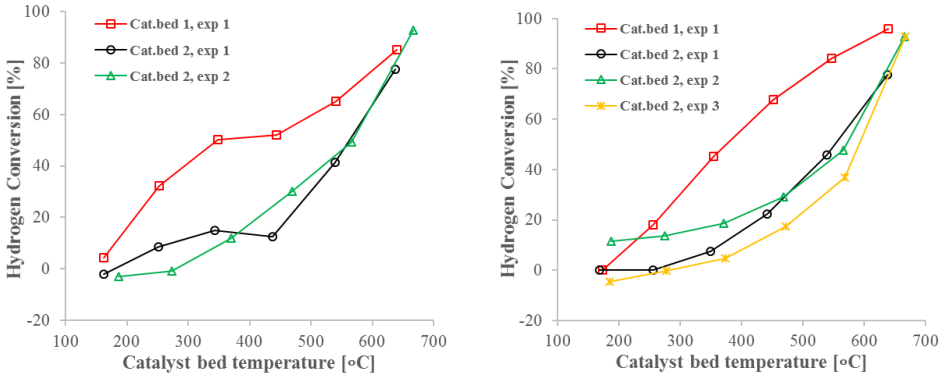

Figure 4.11: Graphs showing the hydrogen conversion plotted against catalyst bed temperature in the hydrogen oxidation experiments (H_2/O_2:1/3). (a): Reactor heating, (b): Reactor cooling.

experiment to observe the temperature gradient and to control where the exothermic reaction is taking place. Temperature profiles and other information related to the experiment are presented in Appendix D.

The experiments were performed with hydrogen (2 mol%) and excess oxygen (6 mol%) in nitrogen and a temperature program as shown in Section 3.3.3, Figure 3.4. All, except for the experiment using Catalyst bed 1, where 1 mol% hydrogen was used, and the temperature was keep at a 30 minute hold every 50 °C. The temperature profiles were measured at every 100 °C. Feed analysis to be used in conversion calculations, and an example of a typical analysis for carbon monoxide oxidation is shown in Appendix B, Table B.1.

Initially, a blank experiment was performed at equal conditions as the experiments with catalyst, without the cooling sequence. The experiment resulted in 11 % conversion of hydrogen at the maximum set point temperature of 700 °C. The graph is shown in Appendix D, Figure D.1 and show a distinct increase in conversion at 400 °C. The temperature profile, in Appendix D, Figure D.2 show the warmest location in the reactor at 20 cm, 613 °C.

Experiments with catalyst were performed as presented in Section 3.3.3, Table 3.4, were two different catalyst beds were used, noted as Catalyst bed 1 and 2. Figure 4.11 present the hydrogen conversion plotted against the catalyst bed temperature for the reactor heating (a) and cooling cycle (b).

Comparing the two graphs in Figure 4.11, the conversion increase with increasing temperatures. During the heating cycle Catalyst bed 1 and 2, Experiment 1, show the same trend (red squares and black circles), even though the conversion is higher for Catalyst bed 1. Both graphs show a flat segment between 300 and 400 °, before the conversion continues to increase, to 85.1 and 77.7 %. The conversion of Catalyst bed 2, Experiment 2 (green triangles), progress similarly to the graphs in the cooling cycle, where the conversion change evenly with the temperature. In the cooling cycle the results are similar, except from the

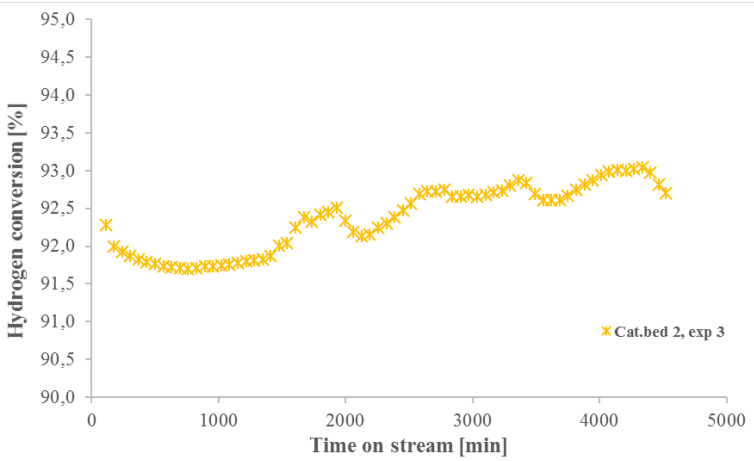

Figure 4.12: Graph showing the H_2 conversion plotted against time on stream for the hydrogen oxidation experiment (H_2/O_2:1/3) which lasted for three days with the oven temperature kept stable at 700 °C.

Table 4.3: Maximum hydrogen conversion for the hydrogen oxidation experiments at the set point temperature of 700 °C.

Experiment	H_2 **conversion at 700 °C [%]**
Catalyst bed 1.1	85.1
Catalyst bed 2.1	77.7
Catalyst bed 2.2	92.9
Catalyst bed 2.3	93.0

experiment with bed 1 (red squares), which again, have a higher conversion than the other experiments. The third experiment performed with Bed 2 (yellow stars) in the cooling cycle follows the three day experiment, and the maximum H_2 conversion is equal to the second experiment using the same Bed of 93 %. Table 4.3 show the maximum conversion for all the experiments at the set point temperature of 700 °C.

In Figure 4.12 the H_2 conversion is plotted against time on stream for the three day experiment at a constant temperature set point of 700 °C, is shown. Over the course of the experiment the hydrogen conversion is stable, fluctuating between 91.7 % and 93.0 % conversion.

The temperature profile was measured at every 100 °C during all the experiments and an example is shown in Figure 4.13, for Catalyst bed 1, Experiment 1. The maximum temperature measured over the catalyst bed is 640 °C, with the oven set point temperature at 700 °C. The profiles for the heating cycle are shown in (a) and reactor cooling cycle in (b), and at all temperature set points above 200 °C, the warmest spot is located between 19 - 21 cm, where the catalyst bed is located. The remaining temperature profiles are shown

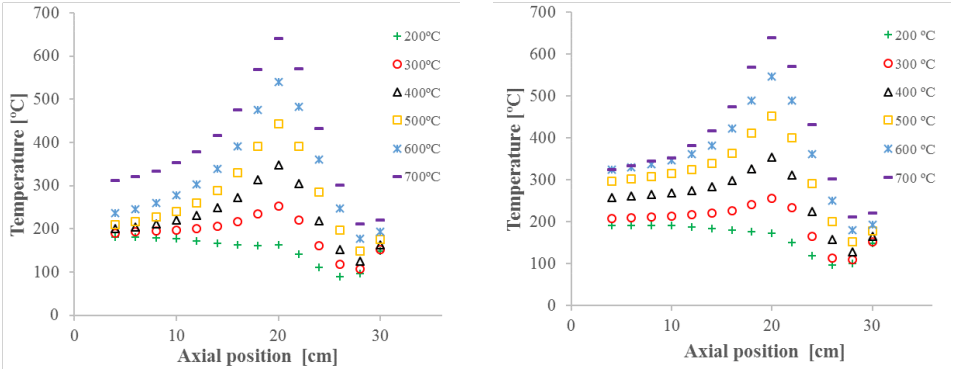

Figure 4.13: Graph showing the temperature profile trough the reactor plotted against the axial position of the thermocouple in a hydrogen oxidation experiment Catalyst bed 1, Experiment 1, for reactor heating (a) and cooling (b) cycle. The catalyst bed is located at 19 - 21 cm.

in Appendix D, Figures D.3 and D.4 and Table D.1.

Mass balance calculations for hydrogen were performed for all experiments to evaluate the accuracy of the measurements made by the gas chromatograph. An example is shown in Figure 4.14 for the experiment performed using Catalyst bed 2, Experiment 1, where the error is plotted against the conversion of hydrogen. The mass balance error decrease with increasing conversing of hydrogen. The remaining mass balances are shown in Appendix D, Figures D.5 to D.7.

4.2.2 Carbon monoxide oxidation

Carbon monoxide oxidation experiments were performed in the MTF set-up to investigate the catalytic activity for the reaction presented in Section 2.1, Equation 2.9. The experiments were performed with polycrystalline silver catalyst, in addition to one reference test without catalyst. For experiments with catalyst the reactor was set up as shown in Section 3.3, Figure 3.3. Temperature profiles over the catalyst bed were measured for each experiment to observe the temperature gradient and to control where the exothermic reaction is taking place. Temperature profiles and other additional information related to the experiment are presented in Appendix D.

The experiments were performed with carbon monoxide (2 mol%) and excess oxygen (6 mol%) in nitrogen and a temperature program as shown in Section 3.3.3, Figure 3.4. The temperature profiles were measured at every 100 °C. Feed analysis to be used in conversion calculations, and an example of a typical analysis for carbon monoxide oxidation is shown in Appendix B, Table B.2.

Initially, a blank experiment was performed at equal conditions as the experiments with catalyst, without the cooling sequence. No carbon dioxide was detected at the maximum

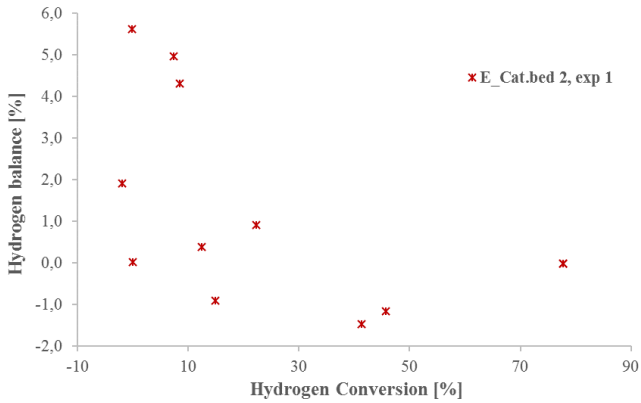

Figure 4.14: Error in hydrogen mass balance plotted against hydrogen conversion in the hydrogen oxidation experiment using Catalyst bed 2, Experiment 1.

set point temperature of 700 °C, which was 615 °C for the warmest spot in the reactor. The temperature profile was measured during the experiment and is shown in Appendix D, Figure D.8 and shows the warmest spot in the reactor to be at 20 cm. This is where the catalyst bed would be located, at 19 - 21 cm.

Experiments with catalyst were performed as presented in Section 3.3.3, Table 3.4, were two different catalyst beds were used, noted as Catalyst bed 1 and 2. Figure 4.15 present the CO conversion plotted against the catalyst bed temperature for the reactor heating (a) and cooling cycle (b).

Comparing the two graphs in Figure 4.15, the conversion increase with increasing temperatures. When heating the reactor the conversion is low until the temperature exceed 500 °C, resulting in a sharp increase, unlike the cooling sequence when the conversion decrease evenly with decreasing temperature. The first experiment for Bed 1 and 2 are similar (red squares and black circles), except for some irregularities, both experiments end with a maximum CO conversion of 68.6 and 69.3 %. For Bed 2, first and second experiment (black circles and green triangles), the maximum conversion decrees from 69.6 % to 46.3 %. The third experiment performed with Bed 2 (yellow stars) is the cooling cycle following the three day experiment, and the maximum CO conversion has decreased further. Table 4.4 show the maximum conversion for all the experiments at the set point temperature of 700 °C.

In Figure 4.16 the CO conversion is plotted against time on stream for the three day experiment at a stable temperature set point of 700 °C. Except for an area with scattered data points, the graph follow a decreasing trend, starting with a conversion of 42.1 % and ending at 9.6 %.

The temperature profile was measured at every 100 °C during all the experiments and an example is shown in Figure 4.17, for Catalyst bed 1, Experiment 1. The maximum temperature measured over the catalyst bed is 635 °C, with the set point temperature of 700 °C.

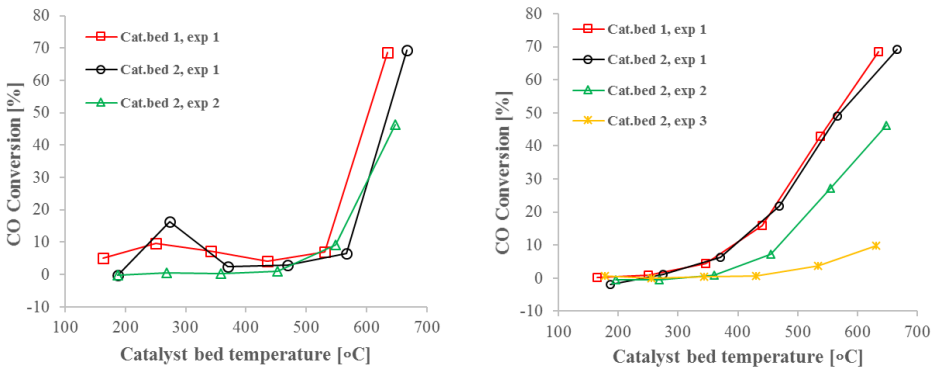

Figure 4.15: Graphs showing the CO conversion plotted against catalyst bed temperature in the carbon monoxide oxidation experiments (CO/O_2:1/3). (a): Reactor heating, (b): Reactor cooling.

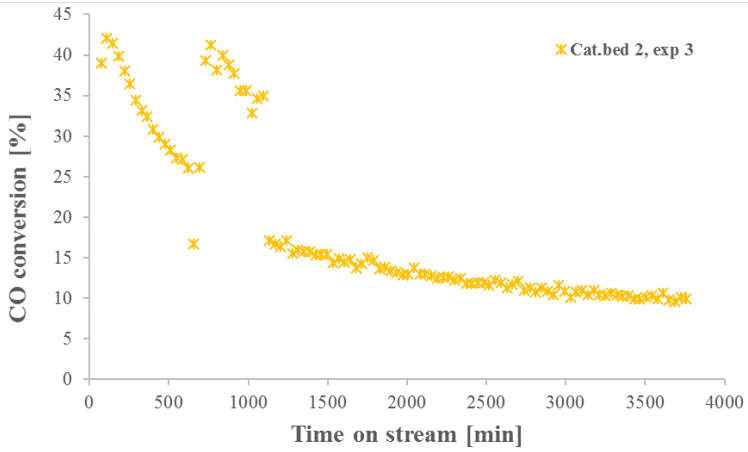

Figure 4.16: Graph showing the CO conversion plotted against time on stream for the carbon monoxide oxidation experiment (CO/O_2:1/3) which lasted for three days with the oven temperature kept stable at 700 °C.

Table 4.4: Maximum CO conversion for the carbon monoxide oxidation experiments at the set point temperature of 700 °C.

Experiment	**CO conversion at 700 °C [%]**
Catalyst bed 1.1	68.6
Catalyst bed 2.1	69.3
Catalyst bed 2.2	41.3
Catalyst bed 2.3	9.1

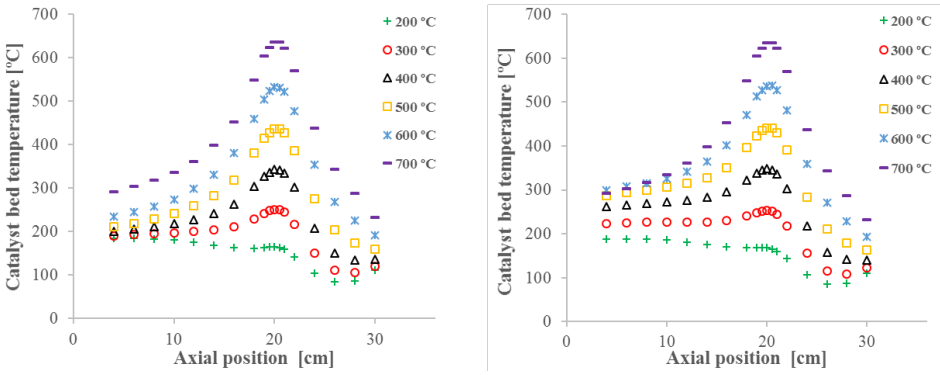

Figure 4.17: Graph showing the temperature profile trough the reactor plotted against the axial position of the thermocouple in a carbon monoxide oxidation experiment Catalyst bed 1, Experiment 1, for reactor heating (a) and cooling (b) cycle. The catalyst bed is located at 19 - 21 cm.

The heating cycle is shown in (a) and reactor cooling cycle in (b), and at all temperature set points above 200 °C, the warmest spot is located between 19 - 21 cm, where the catalyst bed is located. The remaining temperature profiles are shown in Appendix D, Figures D.9 and D.10 and Table D.2.

Mass balance calculations for carbon were performed for all experiments to evaluate the accuracy of the measurements made by the gas chromatograph. An example is shown in Figure 4.18 for the experiment performed using Catalyst bed 1, where the error is plotted against the conversion of carbon monoxide. The mass balance error increase with increasing conversing of carbon. The remaining mass balances are shown in Appendix D, Figures D.11 to D.13.

4.2.3 Methanol oxidation

A methanol oxidation experiment was performed in the MTF set-up to investigate the catalytic activity of polycrystalline silver catalyst. The reactor was set up as shown in Section 3.3, Figure 3.3. Temperature profiles over the catalyst bed were measured for the experiment to observe the temperature gradient and to control where the exothermic reactions are taking place.

The experiment was performed with excess methanol (8.0 mol%) and oxygen (3.5 mol%) in nitrogen and a temperature program as shown in Section 3.3.3, Figure 3.4. The temperature profiles were measured at every 100 °C. The feed analysis used in conversion calculations is shown in Appendix B, Table B.3. Due to experimental equipment malfunction, only one experiment was performed with a reactor heating cycle at temperatures from 200 - 600 °C

Figure 4.19 show the reactant conversions and carbon selectivity plotted against the cata-

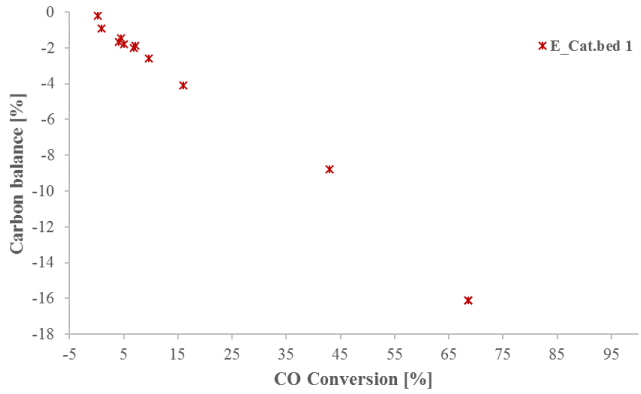

Figure 4.18: Error in carbon mass balance plotted against CO conversion in the carbon monoxide oxidation experiment using catalyst bed 1.

lyst bed temperature. Both reactant conversions, methanol (blue circles) and oxygen (red triangles) increased rapidly at the temperature set point of 300 °C, before stabilising at their respective conversions of about 65 % and 95 %. The selectivities of the carbon products, formaldehyde (yellow stars), carbon monoxide (green diamonds) and carbon dioxide (grey squares) are also shown. Formaldehyde and carbon dioxide selectivity increase with the same rate as the reactants conversion, but formaldehyde continues to increase, where carbon dioxide decrease. According to GC analysis, formic acid was also a product of the reaction, but is not shown here, as the GC was not recently calibrated for formic acid making it difficult to give exact amounts of this product. The trend show an initially high production of the acid, but decreasing with increasing temperature. At the reactor set point temperature of 500 °C, formic acid was no longer detected.

The temperature profile was measured at every 100 °C during the experiment and is shown in Figure 4.20. The maximum temperature measured over the catalyst bed is 560 °C, with the set point temperature of 600 °C. The warmest spot is at 18.5 - 20 cm, where the catalyst bed is located. At the oven set points of 300 °C and 400 °C, the temperature over the catalyst bed exceeded the oven temperature by 70 °C and 25 °C, respectively, indicating highly exothermic reactions taking place.

Table 4.5 show the average carbon mass balance, methanol conversion and catalyst bed temperatures for the experiment. The balance is negative, which indicate more carbon leaving the system is detected then carbon in the feed. The error initially increase with increasing temperature and conversion levels, before it decrease at higher temperatures. Values for formic acid are not included, and may account for the trend in the balance.

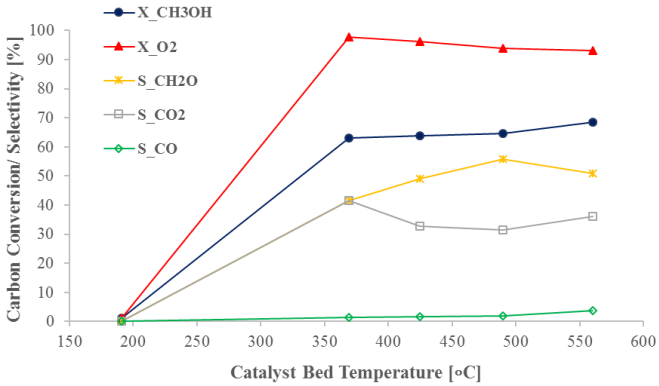

Figure 4.19: Graph showing the conversion of methanol and oxygen, and selectivity towards the carbon products; formaldehyde, carbon monoxide and carbon dioxide in the methanol oxidation experiment (CH_3OH/O_2:2.314 and heating set points 200 - 600 °C).

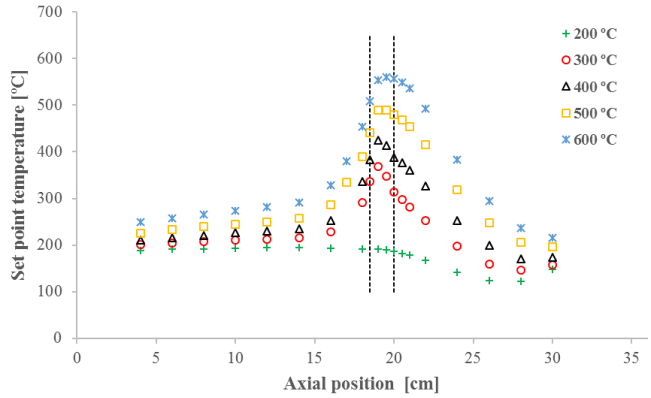

Figure 4.20: Graph showing the temperature profile trough the reactor plotted against the axial position of the thermocouple in the methanol oxidation experiment, for furnace set points 200 - 600 °C. The catalyst bed is located at 18.5 - 20 cm, marked by vertical dotted lines.

Table 4.5: Average carbon mass balance, methanol conversion and catalyst bed temperature for the methanol oxidation experiment.

Catalyst Bed Temperature [°C]	CH3OH Conversion [%]	Carbon Balance Error [%]
191	1.2	-0.3
369	63.0	-9.9
425	64.0	-10.5
490	64.6	-7.1
560	68.6	-6.3

Chapter 5

Discussion

5.1 Catalyst Characterisation

The main purpose of using X-ray diffraction and scanning electron microscopy characterisation was first, to create a base for comparison and learn more about the structure of the silver catalyst. After performing experiments, the techniques were used to provide information of the effect said experiments had on the structure. This information will also be discussed in supplement to the results in its entirety.

5.1.1 X-Ray Diffraction

X-ray diffraction analysis was used on a selection of the silver catalyst samples to investigate the crystalline phases in the silver. The silver was identified as having a face-centred cubic structure by the Diffrac.Eva software database and the narrow, sharp peaks, in Figure 4.1, indicate high crystalline samples [18]. Comparing the samples, some shift in peak intensity is visible. This indicate a phase restructuring in the bulk of the silver. However, for verification, the experiment and analysis should be repeated.

The crystal size was calculated using Diffrac.Eva software and the Scherrer formula, in Equation 2.11. The Scherrer constant, K, is a factor of particle shape. This constant is usually 0.89, but can vary from 0.89 to 1.0, influencing the crystal size. No great change in crystal size was detected, except for a slight decrease in the silver used in oxidation experiments, as presented in Table 4.1. Normally, a catalyst exposed to high temperatures over a longer period of time experience particle growth in the form of sintering. According to Nagy et al., the opposite can occur when silver is heating in the presence of oxygen. Diffused γ-oxygen can substitute for silver lattice atoms and will eventually cause failure in the structure which result in crystal size reduction [29]. Still, an important factor is that

transport and diffusion mechanism in the catalyst is not known and the results can not be verified without further testing.

An important factor in this chase, the XRD method is mainly for gaining information of bulk and not surface structure, indicating these results are best used as indications.

5.1.2 Scanning Electron Microscopy

Micrographs of all silver catalyst samples were analysed to investigate morphological changes in fresh and exposed catalyst.

When using SEM, only a random selection of scan sites are selected, scanned one at a time. Therefor, if the sites reflect the entire sample is uncertain. The technique is also limited as one can only scan the surface, not different angles or inside the particles and the resolution is only valid to a certain magnification. To verify a representative surface, selected samples were analysed on several occasions.

The silver particles show a great variety in the visible surface changes by SEM, as a result of the various atmospheres and reaction conditions compared to the fresh silver, as presented in Section 4.1.2. Comparing the fresh silver, in Figure 4.2, to nitrogen and hydrogen calcinated silver, Figures 4.3 and 4.4, show the greatest similarities. Some topographic changes are evident in the nitrogen and hydrogen treated samples, such as minor hole formation. Nitrogen is present in the system as an inert, not adsorbing or reacting on the surface, making it likely that the changes are a result of thermal energy and minimisation of surface energy. Hydrogen is reported to diffuse into the silver bulk, but when comparing the silver structures, neither time or components present in the gas feed seems to have an effect on the silver morphology in SEM scale, suggesting hydrogen alone also acts as an inert.

Waterhouse et al. used Raman spectroscopy and temperature programmed desorption (TPD) to characterise chemisorbed oxygen species on silver. Results from analysis of the as-received silver catalyst showed presence of subsurface oxygen, identified as β-oxygen [13]. High temperature and trace amounts of subsurface oxygen, or feed gas impurities, seems likely to be the cause of the surface changes in the silver treated with nitrogen and hydrogen.

The silver particles exhibiting a pronounced restructuring of the surface on the mesoscopic scale, are the silver treated with oxygen, both in air and as catalyst for the oxidation experiments. Exposure to synthetic air resulted in massive changes in morphology for all samples, shown in Figure 4.5, though more extensive with time. The micrographs are consistent with results obtained by Waterhouse et al. where polycrystalline silver catalyst was exposed to oxygen for 5 hours at 923 K [13].

Facet formation shown in the SEM images, are in accordance with the increase in inter and surface diffusion occurring in the presence of oxygen and temperatures above the Tammann temperature (345 °C for silver) [13]. Present oxygen is believed to chemisorbe onto the silver surface, lowering the surface free energy, promoting densely packed, (111)

facet termination, and simultaneously incorporate into the silver bulk causing the silver lattice to expand [13].

Silver used as a catalyst for the hydrogen and carbon monoxide oxidation exhibit similar restructuring, independent of the bed has been used for one or multiple experiments, as show in Figures 4.7 and 4.8. A smooth surface with irregular facetted areas and holes are visible. As described by Millar et al. the formation of pinholes are based in the hypothesis that the holes are created by recombination of sub-surface hydroxy species in the silver, especially, close to surface defects [14]. Waterhouse et al. argue the pinholes are formed by reaction between bulk-dissolved β-oxygen and hydrogen [6]. In situ observations were performed of polycrystalline silver, by Millar et al., in steam atmosphere and as a catalyst for a mix of methanol and oxygen. For both reactions, the hole formation rate and size increased with temperature. After, the silver was used in TPD analysis where hydrogen, water and carbon dioxide were detected.

This may indicate that the formation of carbon dioxide also can be the source of pinhole formation, as the SEM micrographs in Figure 4.8 show. The morphology of the holes produced by hydrogen and carbon monoxide oxidation are similar, but if they are structurally equal is unknown. During the first experiment using carbon monoxide the lab experienced a power shortage, how much, and if the catalyst structure was effected is not know, but when comparing with the second bed, the effect seems minimal. Some of the structural changes can also be due to the nitrogen atmosphere used in between experiments for the catalyst bed used for multiple experiments.

The third oxidation experiment, using methanol, showed two different morphological states during SEM analysis, as presented in Figure 4.9. The random sample from the catalyst bed bulk shows little signs of use. This is similar to images from fresh catalyst and the hydrogen calcination, with clear angels and terrace structures. The was unlike the sample from the top of the bed. Here, hole formation is clearly visible, but still lacking the smoothing and grain annealing visible from other oxidation experiments. This may be explained by the short duration of the experiment due to equipment malfunction. The catalyst was only exposed to temperatures close to 600 °C for a short period of time, as the complete experiment lasted for 5 hours. During the experiment the temperatures rose quickly, as shown in the temperature profile in Figure 4.20, promoting exothermic reactions. This may have lead to local hot-spot, normally evened out by the steam in the reactant feed [7]. The reactions on these sites could have contributed to the variations in morphology, producing the holes in the silver surface. As observed by Millar et al., the pinhole production first occurred at temperatures lower then for the steam atmosphere (360 and 440 °C, respectively). The pinholes where also of a greater concentration with methanol present [14].

Last, the experiment performed with a mix of methanol and steam produced no great structure change present in the catalyst (Figure 4.6). This is in contradictory to the, previously mentioned, experiments performed by Millar et al. [14] and coincides with the theory of Waterhouse et al., where the O_β, is key to pinhole formation [6]. More experiments should be performed and repeated SEM analysis should be performed before a conclusion can be drawn.

During the methanol/steam calcination experiment, some activity indicating methanol dehydrogenation was observed by GC analysis (Equation 2.1). It is unknown if the reaction occurred as gas phase or catalytic reaction, but is another indication that atomic oxygen must be present to activate the silver surface for both structural changes and reactions, such as methanol dehydrogenation reaction, where oxygen is not directly involved in the reaction [9]. A general comparison of the micrographs representing silver exposed to atmospheres with and without oxygen in the feed, indicate that oxygen seems to be the main cause of morphological structure changes for experiments performed in this study.

The silver catalyst experience great structural change during the start up of formaldehyde synthesis and influence both product formation and formaldehyde selectivity. Understanding what effects the structure and activity can be important in the work of understanding and improve the silver catalyst for formaldehyde production [3, 6].

5.2 Catalyst Activity

Side reactions, gas phase reactions, changes in catalyst morphology and activity are among some of the challenges in the formaldehyde process. Catalytic reactions were performed to investigate reaction pathways and catalyst activity. Further, the results from oxidation experiments will be discussed.

The experiments were performed in the MTF set-up were temperature and gas composition were the variable conditions. To have better control of the reaction temperatures, the silver catalyst were set up with a quartz sinter and wool as support. For all the experiments performed, the reactive system has not been at steady state, as the experiments being performed are meant to represent the start up of a process using fresh catalyst. As the catalyst restructure, the process will not reach steady state during the time scale of these investigations. Temperature profiles were measured for every experiment. This was performed manually, and will represent an uncertainty. Both placement of the thermocouple and the time of the measurement may have influenced the values.

5.2.1 Hydrogen Oxidation

Hydrogen oxidation using hydrogen (2 mol%) and excess oxygen (6 mol%), was performed using two different catalyst beds. Initially a blank experiment was performed to investigate gas phase reactions. Results from the gas chromatograph showed detection of H_2O, indicating that at a set point of 700 °C and a temperature of 613 °C measured in the reactor, were sufficient to oxidise hydrogen to some extent (Appendix D, Figure D.1). Temperature profile was measured at every 100 °C (Appendix D, Figure **??**) and show the warmest location along the reactor at 20 cm, which was the location of the quartz sinter.

The first experiment, using catalyst bed 1, was performed under sightly different conditions then the remaining experiments. A lower amount of hydrogen (1 mol%) was used with the same amount of silver catalyst, in addition to the temperature program variations.

The difference in the ratio between reactant and catalyst might be the cause of the higher conversion levels at intermediate temperatures, shown in Figure 4.11, both in the heating and cooling cycle.

Comparing the first experiments for catalyst bed 1 and 2, a flat segment between 350 °C and 450 °C is noticeable for both experiments. This coincide with the Tammann temperature of silver and is according to Waterhouse et al. [13] where silver restructuring is activated by increased bulk mobility for the silver atoms. The change in silver morphology, is a result of inter and surface diffusion, and enable incorporation of oxygen and hydrogen into the bulk. As the oven temperature continues to increase, the promotion of active oxygen species occurs and hydrogen conversion rise. Seen in connection with the SEM analysis, massive morphological changes are visible, such as pinholes and facet termination.

The catalyst bed, used in several experiments, shows increased conversion with time, as shown in Table 4.3. This may indicate a silver catalyst restructuring which promotes hydrogen oxidation. The conversion was stable over a longer period of time in the third experiment (3 days), indicating the initial restructuring is somewhat stabilised, to the point there it no longer effect the reactivity of hydrogen (Figure 4.12). The silver samples used for one experiment exhibit equal topology as silver used in several experiments, on the scale provided by SEM analysis. This suggest the restructuring happens rather quickly, in the time scale of the formaldehyde synthesis start up, which is said to last for periods up to a week until steady-state is reached. The structure observed in this work is similar to that shown in similar research [14, 9].

The mass balance error is larger then what is within reason for sections of the experiments, decreasing the reliability of the results (Figure 4.14). From past experience, the GC does not perform satisfactory water analysis. During the period of the experiments, measures were taken to improve the analysis and the mass balance error, resulting in slightly improved results. Conversion is therefor calculated based on reacted hydrogen, not produced water.

The experiment using catalyst bed 2, second experiment, the temporary stay in temperature was shorter then for the other experiments. This variation may have been made visible by the increased conversion at the end of the cooling cycle, suggesting the system did not have sufficient time to adapt to the change in temperature. Temperature profiles are similar for all experiments, where the warmest location is measured in the area of the catalyst bed and support the oxidation occurring as catalytic reaction and not as gas phase reaction.

The results clearly shows hydrogen oxidation to be an active reaction on the silver catalyst, in addition to be a source of catalyst restructuring. Also, the reaction is capable of competing for the oxygen in the formaldehyde synthesis.

5.2.2 Carbon Monoxide Oxidation

Oxidation of carbon monoxide (2 mol%) and excess oxygen (6 mol%), was performed using two different catalyst beds. Initially a blank experiment was performed to investigate

gas phase reactions. Temperature profile at every 100 °C were measured and are shown in Appendix D, Figure D.8. The graph show the warmest spot along the reactor at 20 cm, which was the location of the quartz sinter.

Results from the gas chromatograph showed no detection of CO_2, indicating that at a set point of 700 °C and a temperature of 615 °C measured in the reactor, was not sufficient to oxidise carbon monoxide. This is consistent with the research done by Ekholdt, where COMSOL simulations of gas phase carbon monoxide oxidation were performed at process conditions relevant to formaldehyde synthesis [30].

Further, experiments using silver catalyst were performed. All experiments were executed equally, but the experiment using catalyst bed 1 experienced a power shortage half way in the experiment. Comparing the conversion data with the other relevant experiment, it does not seem to have much impact on the results. Experiment 1 for catalyst bed 1 and 2, show great likeness and reproducibility, ending with similar conversion at maximum temperatures, as listed in Table 4.4.

Figure 4.15 show the conversion of carbon monoxide plotted against the catalyst bed temperature, during reactor heating and cooling cycle. All experiments show the same behaviour during the heating cycle, with low conversion of carbon monoxide until sufficient temperature is reached, and the conversion increase rapidly. This is evident also for the catalyst bed used for multiple experiments. The conversion results in the cooling cycle follow a trend, but not equal to the heating cycle. The maximum conversion of carbon monoxide decrease as the catalyst bed is submitted to continued process conditions. This is clearly shown in Figure 4.16, where the conversion is reduced from 41 % to 9 % over the course of three days at approximately 630 °C over the catalyst bed. The scattered points on this graph is most likely caused by pressure variations in the GC analysis, resulting in different amounts of gas in the injection loop. The pressure change was caused by precipitation in the water-lock located on a parallel pipeline to the GC. The precipitation was removed at the time where the data points continue to follow the decreasing trend.

Carbon mass balance graphs show the same trend, where the error increase with increasing carbon monoxide conversion, which indicate a uncertainty in the GC analysis for low amounts of reactant.

The temperature profiles are similar for all experiments showing the warmest location the catalyst bed at the position of the catalyst bed, indicating the exothermic reactions occur on the bed and not as gas phase reactions.

These results correlate with the observations made by Qu et al., and silver is an active catalyst for carbon monoxide oxidation [15]. A hypothesis to explain the trends shown between heating and cooling cycles may indicate that carbon monoxide have similar influence on silver as on platinum crystals, described by Van Santen [16]. The carbon monoxide activates the platinum surface, restructuring the phase form a stable, dense, (111) structure to an open, more active (100) structure, which promote carbon dioxide formation.

The results also indicate that the activity is not maintained over time. This may be caused by silver restructuring, permanently shifting towards the (111) structure, being the thermodynamically favourable structure for silver. Comparing with the XRD results, an increased

intensity for the (111) structure is observed in the diffractrogram for the silver used in carbon monoxide oxidation, in Figure 4.1, compared to the fresh silver.

Carbon loss in the formaldehyde synthesis is mostly caused by selectivity towards the main byproduct, carbon dioxide, and understanding how to avoid this could be of great use to increase formaldehyde production. Results from this work indicate that after sufficient silver catalyst restructuring, the carbon dioxide source does not seem to generate from the reaction between carbon monoxide and oxygen. Also, the oxidation reaction would not be a competing reaction for oxygen consumption.

5.2.3 Methanol Oxidation

Only one methanol oxidation experiment was performed due to equipment failure. The experiment was performed by feeding methanol (8 mol%) in excess and oxygen (3.5 mol%). No water was added to the reactant feed, which is common in formaldehyde synthesis. The methanol/ oxygen ratio was between the needed values for partial and total oxidation of methanol, Equations 2.2 and 2.3.

Figure 4.19 show the conversion of methanol and oxygen, in addition to the carbon selectivity's. Both conversion of methanol and oxygen increase rapidly at temperatures reaching 370 °C, and can be experienced as the "light-off", where the silver catalyst begins an initialisation phase, as described by Nagy [12]. Bulk-diffusion by β-oxygen was observed at temperatures above 300 °C. The oxygen diffuse along grain bounties and surface defects in the silver catalyst, activating restructuring.

As shown in the temperature profile in Figure 4.20, the catalyst bed temperature increase above the oven set point in correlation with the light-off temperature. This indicate highly exothermic reactions are taking place, such as partial and total oxidation of methanol and formaldehyde, show in Section 2.1. This elevated temperatures may also have lead to carbon deposition on the catalyst bed, explaining the black spots on the catalyst, as show in Figure 4.10. The EDX analysis confirmed the presence of carbon and oxygen on the catalyst, but can not confirm if it was a result of coke or a carbon species introduced to the silver surface after the experiment was carried out (Table 4.2). SEM analysis show local morphological changes on the catalyst similar to results shown for other oxidation experiments, being exposed to high temperatures for a longer period of time. The comparison may indicate active catalyst sites and local hot spots on the catalyst.

Initially, formic acid was detected by the GC analysis. The amount decreased as the temperature rose, and was no longer present at 500 °C. Formic acid is not shown as a part of the results, because the GC method was not calibrated for the compound, making quantitative analysis challenging. This provides an additional error in the mass balance for carbon, hydrogen and oxygen, resulting in only the carbon balance being presented (Table 4.5). The balance error is higher then the allowed 5 %, which is expected, but decrease with temperature, when formic acid levels fall. Conversion and carbon selectivity is therefor calculated on the basis of methanol reacted, and not product levels.

Research on comparing formaldehyde synthesis with and without water vapour in the re-

action gas was performed by Qian et al. [7], Results showed an increased conversion of methanol and formaldehyde selectivity with the water ballast method. Light off at 300 °C and increased production of formic acid at low temperatures when water was excluded from the reaction gas, correlating with the present results. Also, carbon dioxide selectivity was higher at lower temperatures and the absence of steam.

The initial carbon dioxide production decrease with temperature. As shown in previous results, the carbon dioxide is not likely to be a product from carbon monoxide oxidation, as the reaction does not seem to be favoured at temperatures bellow 500 °C for near fresh silver catalyst.

The reaction did not achieve full oxygen conversion (max. 97.8 %). This is surprising, as the oxygen was not feed in excess and participates in several reactions, including hydrogen oxidation presented in the current work. Bao et al. state, water and hydroxy must be present to promote surface restructuring of the silver and formation of γ-oxygen, relevant for methanol oxidation and formaldehyde selectivity at elevated temperatures [8]. Strongly bound γ-oxygen is associated with exclusively partial oxidation of methanol to formaldehyde. The work by Bao et al., indicate that producing bound γ-oxygen from hydroxy reaction is more favourable then by electron donation from the silver metal. When water is removed this will increase the barrier for γ-oxygen to be formed, also increasing the chance of oxygen desorbing from the silver surface forming oxygen molecules. The experiments should be completed and reproduced before conclusions can be drawn, but the theory gives rise to the idea of repeating hydrogen and carbon monoxide oxidation experiments with steam to investigate the effect.

Formaldehyde could react with oxygen, downstream of the reactor, but with elevated gas velocity and sufficient cooling after the reactor, oxygen detection in the product gas might be explained.

Chapter 6

Conclusion

In this master thesis, polycrystalline silver catalyst have been used to investigate catalytic activity and the effected of different atmospheres on the morphological structure of the catalyst relevant to the formaldehyde synthesis. The motivation for the project was to contribute to the continued development and understanding of the silver catalyst technology used in formaldehyde production.

The silver catalyst was exposed to various conditions to investigate the dependency between the conditions and catalyst structure, analysed by SEM and XRD. Conditions, such as time dependency, temperature and atmosphere compositions were used to gather information about the interaction between silver and various components present in the experiments. Further, the effect of catalytic oxidation reactions were tested in the connection with activity data.

The XRD diffraction confirmed the presence of highly crystalline fcc silver and a shift in the crystalline base plane structures after use. SEM investigations indicated that the silver particles were effected differently based on the process conditions. At 650 °, thermal energy was the main driving force causing signs of restructuring in the silver exposed to nitrogen and hydrogen atmospheres, independent of the exposure time. This was also the case with exposure to methanol and steam in nitrogen, where in addition, only trace amounts of produced formaldehyde and hydrogen was detected.

Morphological changes in the silver was observed when oxygen was present. Silver calcined in air showed increasing restructuring with time, eliminating angular grain structure, production of pinholes and promoting irregular and smooth facet formation. Using the silver as a catalyst for hydrogen, carbon monoxide and methanol oxidation resulted in the same observations.

It was found that the silver catalyst display high catalytic activity for hydrogen oxidation, facilitated by catalytic restructuring towards increased conversion of hydrogen. The catalyst displayed an initial catalytic activity for carbon monoxide oxidation which declined

over time. Equal morphological changes were observed on the mesoscale, suggesting the restructured silver promotes hydrogen oxidation, as opposed to carbon monoxide oxidation. This indicate the oxidation of hydrogen to be a competing reaction for oxygen in the formaldehyde synthesis. Performing oxidation of methanol without water, promoted the essential role of water in the reaction, in connection with temperature control and product selectivity.

In general, oxygen displays an important role promoting and activating reactions and influence the silver catalyst morphology. This is especially critical for silver catalyst activation and performance during process start-up in the formaldehyde production.

Chapter 7

Further work

In this work, only a few methods for silver characterisation was used. The project work could have benefited from using more surface sensitive techniques to gain a better understanding of the silver surface structure and properties. Advanced characterisation methods, such as STM, TEM, Raman, AFM and Krypton BET could be beneficial.

Operating the MTF set-up, some challenges arose. The experimental result could benefit from changing flow and liquid controllers more suited to the feed interval, to increase feed precision. Also, a calibration of formic acid is required. To improve the product stream analysis, using GC combined with MS or switch to IR detection could be promising.

Further investigating the reaction pathways and silver restructuring should be investigated to gain a better understanding of the catalytic system. Experiments, such as calcination of silver in water, and CO, continuing methanol oxidation experiments with and without water, and using equal conditions as for hydrogen and CO oxidation performed in the work, would be interesting. To get a better understanding of how water effect the formaldehyde process, the current experimental work could be repeated with added steam.

As previously mentioned, the catalyst structure varies from start-up and at steady-state conditions. By performing experiment with pre-calcinated silver it could provide information about how the start-up phase of the experiments is effected.

Bibliography

[1] I. Business Wire. (2011, May) Annual consumption growth of 5 % expected on formaldehyde market according to merchant research & consulting, ltd. [Online]. Available: https://www.businesswire.com/news/home/20110526005760/en/Annual-Consumption-Growth-5-Expected-Formaldehyde-Market

[2] A. W. Franz, H. Kronemayer, D. Pfeiffer, R. D. Pilz, G. Reuss, W. Disteldorf, A. O. Gamer, and A. Hilt. (2016, November) Ullmann's encyclopedia of industrial chemistry, formaldehyde. [Online]. Available: http://onlinelibrary.wiley.com/doi/10.1002/14356007.a11_619.pub2/abstract

[3] G. Millar and M. Collins, "Industrial production of formaldehyde using polycrystalline silver catalyst," *Industrial and Engineering Chemistry Research*, vol. 56, no. 33, pp. 9247–9265, August 2017.

[4] C. D. NTNU. (2017) icsi - industrial catalysis science and innovation. [Online]. Available: https://www.ntnu.edu/icsi

[5] J. A. Moulijn, *Chemical process technology*, 2nd ed. Chichester: Wiley, 2013.

[6] G. I. Waterhouse, G. A. Bowmaker, and J. B. Metson, "Influence of catalyst morphology on the performance of electrolytic silver catalysts for the partial oxidation of methanol to formaldehyde," *Applied Catalysis A, General*, vol. 266, no. 2, pp. 257–273, 2004.

[7] M. Qian, M. Liauw, and G. Emig, "Formaldehyde synthesis from methanol over silver catalysts," *Applied Catalysis A, General*, vol. 238, no. 2, pp. 211–222, 2003.

[8] X. Bao, M. Muhler, B. Pettinger, Y. Uchida, G. Lehmpfuhl, R. Schlögl, and G. Ertl, "The effect of water on the formation of strongly bound oxygen on silver surfaces," *Catalysis Letters*, vol. 32, no. 1, pp. 171–183, March 1995.

[9] G. I. Waterhouse, G. A. Bowmaker, and J. B. Metson, "Mechanism and active sites for the partial oxidation of methanol to formaldehyde over an electrolytic silver catalyst," *Applied Catalysis A, General*, vol. 265, no. 1, pp. 85–101, 2004.

[10] I. E. Wachs and R. J. Madix, "The oxidation of methanol on a silver (110) catalyst," *Surface Science*, vol. 76, no. 2, pp. 531–558, 1978.

[11] A. Andreasen, H. Lynggaard, C. Stegelmann, and P. Stoltze, "Simplified kinetic models of methanol oxidation on silver," *Applied Catalysis A, General*, vol. 289, no. 2, pp. 267–273, 2005.

[12] A. Nagy, G. Mestl, T. Rühle, G. Weinberg, and R. Schlögl, "The dynamic restructuring of electrolytic silver during the formaldehyde synthesis reaction," *Journal of Catalysis*, vol. 179, no. 2, pp. 548–559, October 1998.

[13] G. I. Waterhouse, G. A. Bowmaker, and J. B. Metson, "Oxygen chemisorption on an electrolytic silver catalyst: a combined tpd and raman spectroscopic study," *Applied Surface Science*, vol. 214, no. 1, pp. 36–51, 2003.

[14] G. J. Millar, M. L. Nelson, and P. J. R. Uwins, "In situ observation of structural changes in polycrystalline silver catalysts by environmental scanning electron microscopy," *Journal of the Chemical Society, Faraday Transactions*, vol. 94, no. 14, pp. 2015–2023, 1998.

[15] Z. Qu, M. Cheng, W. Huang, and X. Bao, "Formation of subsurface oxygen species and its high activity toward co oxidation over silver catalysts," *Journal of Catalysis*, vol. 229, no. 2, pp. 446–458, 2005.

[16] R. A. Sheldon and R. A. v. Santen, *Catalytic oxidation: principles and applications - a course of the netherlands institute for catalysis research (niok)*. World Scientific Pub Co Pte, October 1995.

[17] B. Viswanathan, *Catalysts and surfaces : characterization techniques*. Oxford: Alpha Science International, 2010.

[18] I. Chorkendorff, *Concepts of modern catalysis and kinetics*, 2nd ed. Weinheim: Wiley-VCH, 2007.

[19] K. W. Kolasinski, *Surface science : foundations of catalysis and nanoscience*. Chichester: Wiley, 2002.

[20] W. D. Callister, *Materials science and engineering*, 8th ed. Hoboken, N.J: Wiley, 2011.

[21] J. Niemantsverdriet, *Spectroscopy in catalysis : an introduction*, 3rd ed. Weinheim: Wiley-VCH, 2007.

[22] J. M. Thomas, *Handbook for Heterogeneous Catalysis. 2., completely revised and enlarged Edition. Vol. 1–8. Edited by G. Ertl, H. Knözinger, F. Schüth, and J. Weitkamp*. Wiley-VCH, Weinheim, 2008.

[23] T. Greibrokk, *Kromatografi : separasjon og deteksjon*, 3rd ed. Oslo: Universitetsforlaget, 1994.

[24] C. F. Poole, *Gas chromatography*, 1st ed. Amsterdam: Elsevier, 2012.

[25] A. Technologies. (2018) Cp-sil 5 cb capillary column. [Online]. Available: https://www.agilent.com/en/products/gas-chromatography/gc-columns/capillary/cp-sil-5-cb

[26] J. T. Richardson, *Principles of catalyst development*, ser. Fundamental and applied catalysis. New York: Plenum Press, 1989.

[27] T. E. C. Industry. (2007) "catalyst science and technology, http://nptel.ac.in/courses/". [Online]. Available: http://nptel.ac.in/courses/103103026/7

[28] H. S. Fogler, *Elements of chemical reaction engineering*, 5th ed., ser. Prentice-Hall international series in the physical and chemical engineering sciences. Boston: Prentice Hall, 2016.

[29] A. Nagy and G. Mestl, "High temperature partial oxidation reactions over silver catalysts," *Applied Catalysis A, General*, vol. 188, no. 1, pp. 337–353, 1999.

[30] R. J. Ekholdt, "Oxidation of methanol to formaldehyde over ag," Master's thesis, Norwegian University of Science and Technology, 2017.

Appendix

Appendix A

Methanol to formaldehyde test set-up

This Appendix contain details about selected equipment in the MTF set-up. Details regarding the reactor design is presented in Figure A.1 and the GC automatic valve injection system is shown in Figure A.2.

All the flow controllers were calibrated either during the specialization project (TKP 4580) or the period of the master thesis. A description of the calibration method is presented in Chapter 3.3.1 and the resulting graphs are presented in this Appendix.

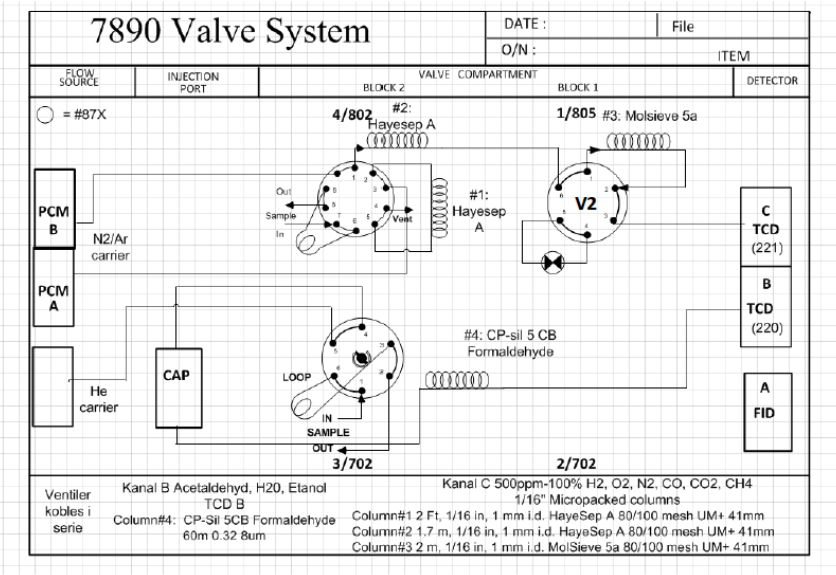

Figure A.1: Valve system controlling GC injections.

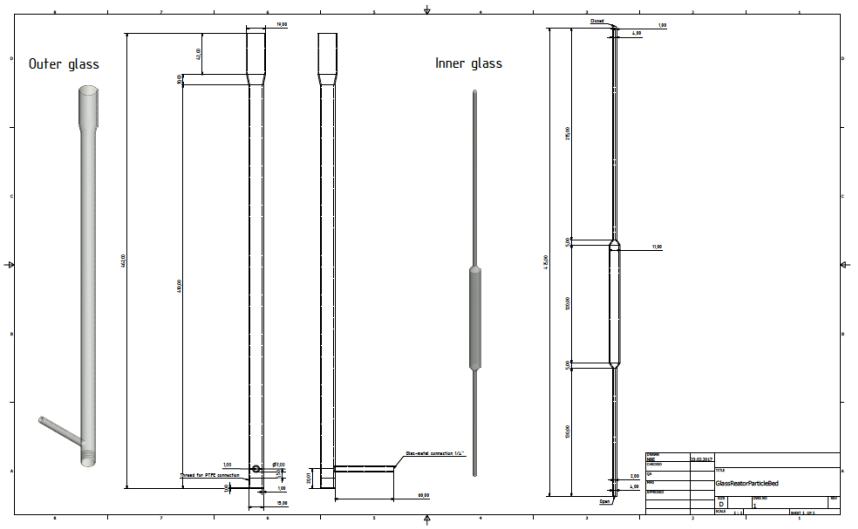

Figure A.2: Reactor details for experiments in the MTF test set-up with particular silver.

Calibration curves

Mass and liquid flow controllers were calibrated using a bobble column and gravimetric method, respectably. Figures A.3 to A.10 show the calibration curves for both nitrogen supply lines (low and high area), air, CO/H_2 and liquid controller feeding pure methanol and a methanol/water mix.

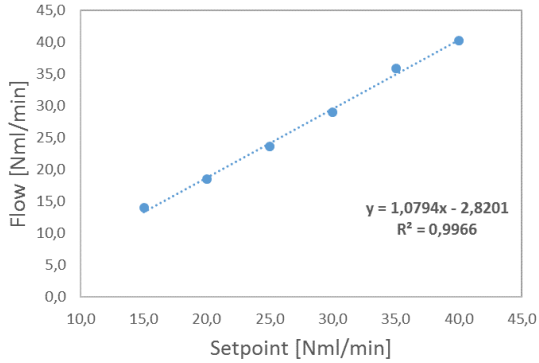

Figure A.3: Calibration curve for nitrogen MFC, line 1, low area.

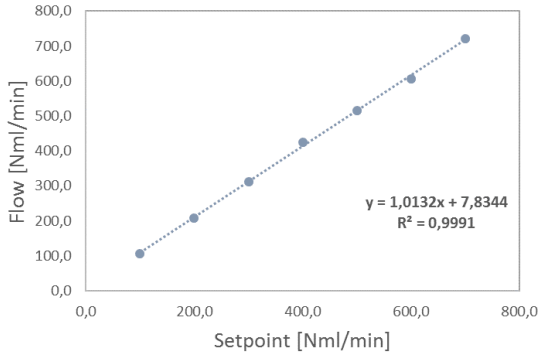

Figure A.4: Calibration curve for nitrogen MFC, line 1, high area.

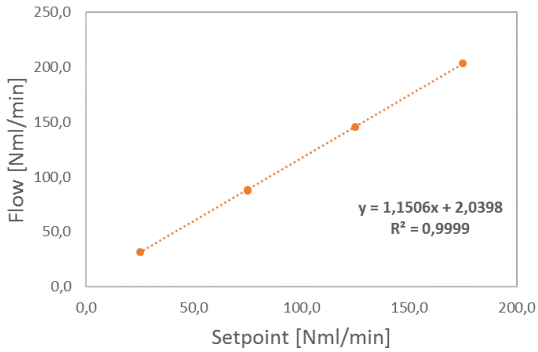

Figure A.5: Calibration curve for nitrogen MFC, line 2

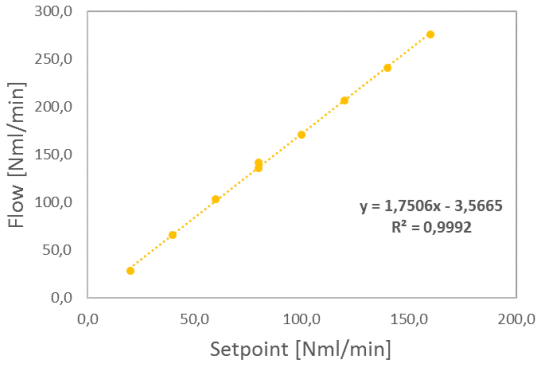

Figure A.6: Calibration curve for air MFC.

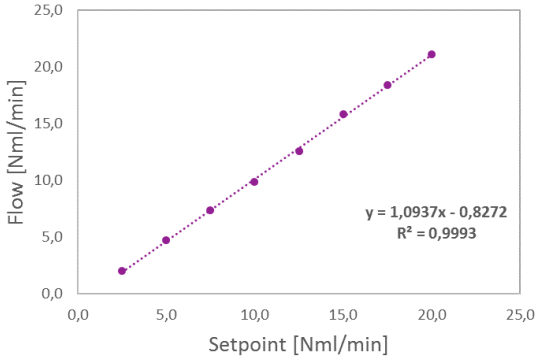

Figure A.7: Calibration curve for carbon monoxide MFC.

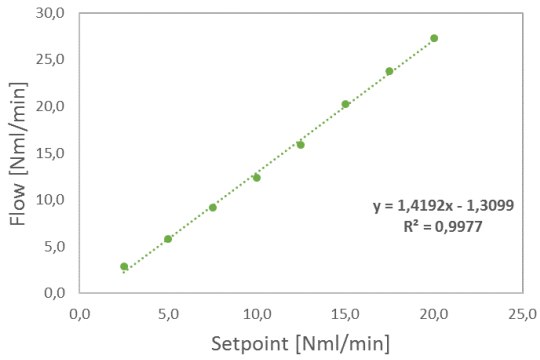

Figure A.8: Calibration curve for hydrogen MFC.

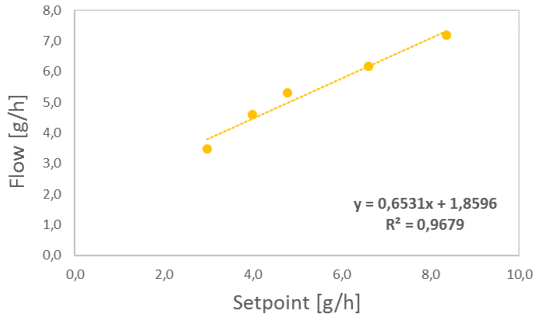

Figure A.9: Calibration curve for LFC feeding methanol.

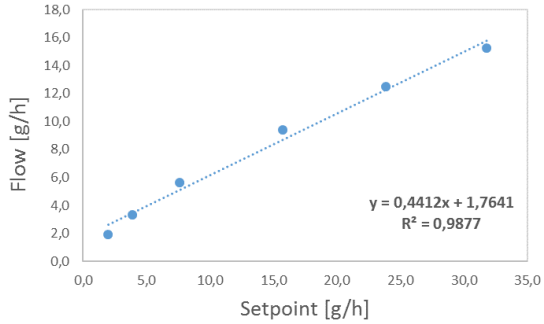

Figure A.10: Calibration curve for LFC feeding a mix of methanol and water.

Appendix B

Feed Analysis

Feed analysis were performed for all activity experiments. Examples are shown in Tables B.1 - B.3. The average values are used further in conversion, selectivity and mass balance calculations.

Table B.1: Feed analysis for a hydrogen oxidation experiment with 2 mol% H_2 and excess oxygen (6 mol%).

Experiment	Hydrogen	Oxygen	Nitrogen
H_2 oxidation, with catalyst	2.5906	6.0270	93.2632
	2.5838	6.0408	93.2354
	2.5795	6.0468	93.2700
	2.5689	6.0421	93.3594
	2.5633	6.0284	93.2318
	2.5646	6.0487	93.3647
	2.5542	6.0507	93.3455
	2.5587	6.0346	93.3239
Average	2.5705	6.0399	93.2992

Table B.2: Feed analysis for a carbon monoxide oxidation experiment with 2 mol% CO and excess oxygen (6 mol%).

Experiment	Carbon Monoxide	Oxygen	Nitrogen
CO oxidation, with catalyst	2.7275	5.9657	93.0092
	2.7377	5.9592	92.9090
	2.7560	5.9863	93.0544
	2.7218	6.0124	93.0604
	2.7512	6.0344	93.0518
	2.7550	6.0261	93.0380
Average	2.7415	5.9973	93.0205

Table B.3: Feed analysis for methanol oxidation experiment with MeOH/O_2:2.314 ratio.

Experiment	Methanol	Oxygen	Nitrogen
MeOH oxidation, with catalyst	6.6160	3.3713	88.5235
	6.7892	3.4003	89.4285
	6.5792	3.3847	88.8120
	6.3204	3.3969	89.1759
	6.6511	3.4541	89.2488
	6.6926	3.5819	88.8551
	6.9780	3.6133	87.9802
Average	6.6609	3.4575	88.8606

Appendix C

Calculations

For all activity experiments the data was further processed using Microsoft Excel. Examples showing the calculations are shown in this Appendix. The calculations are based on the equations shown in Chapter 3.3.4.

Calculating the conversion of, for example hydrogen, X_{H_2}, is done using Equation C.1,

$$\mathrm{X_{H_2}} = 1 - \frac{\mathrm{y_{H_2,out}}}{\mathrm{y_{H_2,in}}} \frac{\mathrm{y_{N_2,in}}}{\mathrm{y_{N_2,out}}} \cdot 100\% \tag{C.1}$$

where $y_{x_{in}}$ are the element values based on the feed analysis and $y_{x_{out}}$ are the element values based on the GC analysis.

$$\mathrm{X_{H_2}} = 1 - \frac{0.61}{2.57} \frac{93.3}{94.58} \cdot 100\% = 76.7\% \tag{C.2}$$

The product selectivity is calculated based on the amount of reacted methanol, using Equation C.3 and formaldehyde as an example, in Equation C.4.

$$\mathrm{S_{CH_2O}} = \frac{\mathrm{F_{Tot,out} y_{CH_2O,out}}}{\mathrm{F_{Tot,in} y_{CH_3OH,in}} - \mathrm{F_{Tot,out} y_{CH_3OH,out}}} \tag{C.3}$$

$$\mathrm{S_{CH_2O}} = \frac{520.7 \cdot 2.28}{500.0 \cdot 6.50 - 520.7 \cdot 1.83} \cdot 100\% = 51.2\% \tag{C.4}$$

The mass balance is used to control the reliability of the GC values and calculations. The mass balance for hydrogen, E_H, is done using Equation C.5,

$$\mathrm{E_H} = \frac{\mathrm{F_{Tot,out}} \sum \mathrm{n \cdot y_{H,out}} - \mathrm{F_{Tot,in}} \sum \mathrm{n \cdot y_{H,in}}}{\mathrm{F_{Tot,in}} \sum \mathrm{n \cdot y_{H,in}}} \cdot 100\% \tag{C.5}$$

where $F_{Tot,out}$ is the total flow calculated based on the inert nitrogen entering and leaving the system, $F_{Tot,in}$ is the total inlet flow, $y_{H,out}$ is the fraction of the elements containing hydrogen leaving the reactor, $y_{H,in}$ is the inlet fraction of elements containing hydrogen based on the feed analysis and n is the stoichiometric factor.

$$\mathrm{E_H} = \frac{246.61(2.01 + 0.61) - 250.00 \cdot 2.56}{250.00 \cdot 2.56} \cdot 100\% = 0.37\% \tag{C.6}$$

Appendix D

Oxidation Experiments

D.1 Hydrogen Oxidation

Additional information and results from hydrogen oxidation experiments are shown in this section.

The graph showing conversion data for the blank experiment is shown in Figure D.1.

Temperature profiles over the catalyst bed were measured for each experiment to measure the temperature gradient and to control where the exothermic reactions are taking place. The profiles are shown in Figures D.3 and D.4 and Table D.1.

The mass balance error for hydrogen was calculated for each hydrogen oxidation experiment to assess the accuracy of the GC analysis and is shown in Figures D.5 to D.7 for experiments using catalyst bed 1 and bed 2, experiments 2 and 3.

Table D.1: Temperatures trough the reactor at 20.5 cm axial position compared to the temperature set point for the carbon monoxide oxidation experiment catalyst bed 2, experiment 3, cooling cycle following the three day experiment. The catalyst bed is located at 19 - 21 cm.

Set point temperature [°C]	**Temperature at 20.5 cm axial position**
200	185
300	277
400	374
500	472
600	569
700	668

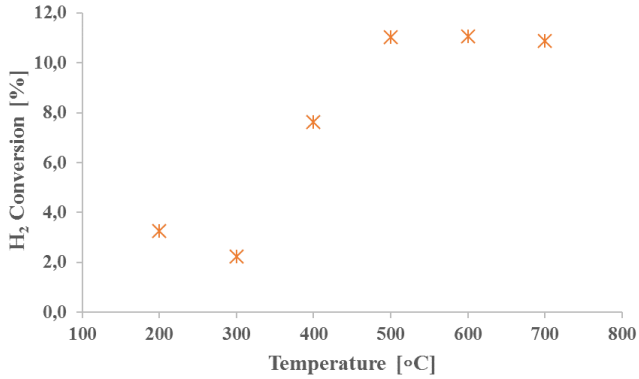

Figure D.1: Graph showing the conversion plotted against set point temperature in the blank hydrogen oxidation experiment.

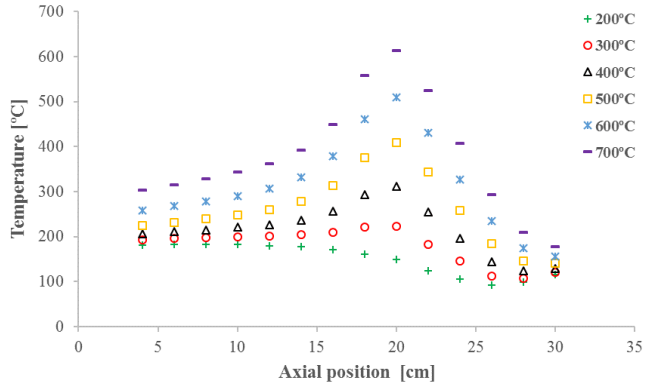

Figure D.2: Graph showing the temperature profile trough the reactor plotted against the axial position of the thermocouple in the blank hydrogen oxidation experiment, for reactor heating. The catalyst bed would be located at 19 - 21 cm.

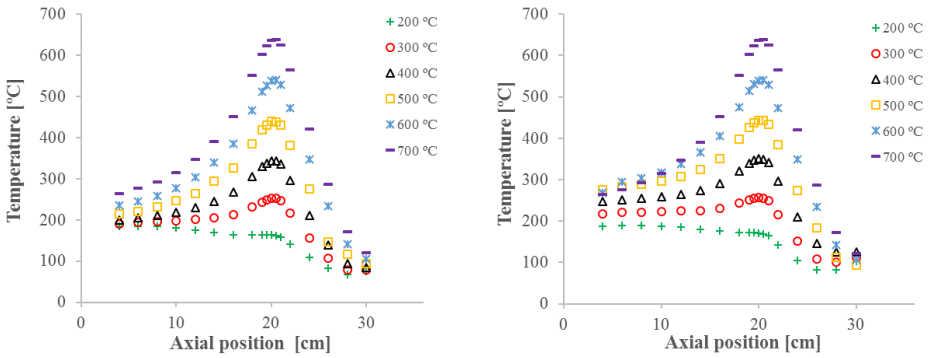

Figure D.3: Graph showing the temperature profile trough the reactor plotted against the axial position of the thermocouple in the hydrogen oxidation experiment catalyst bed 2, experiment 1, for reactor heating (a) and cooling (b) cycle. The catalyst bed is located at 19 - 21 cm.

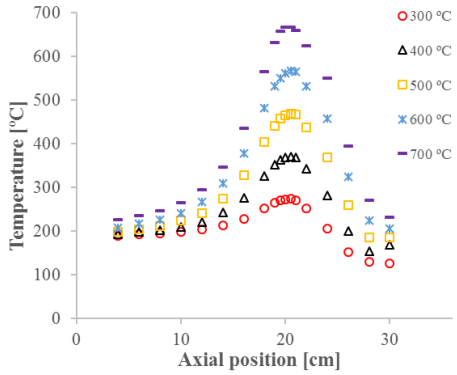

Figure D.4: Graph showing the temperature profile trough the reactor plotted against the axial position of the thermocouple in the hydrogen oxidation experiment catalyst bed 2, experiment 2, for reactor heating (a) and cooling (b) cycle. The catalyst bed is located at 19 - 21 cm.

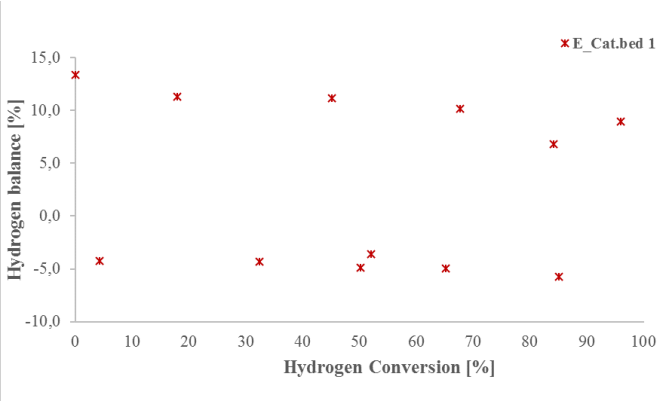

Figure D.5: Error in hydrogen mass balance plotted against hydrogen conversion in the hydrogen oxidation experiment using catalyst bed 1, experiment 1.

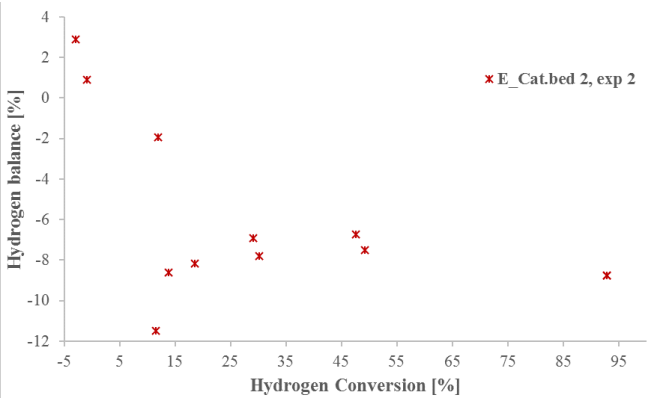

Figure D.6: Error in hydrogen mass balance plotted against hydrogen conversion in the hydrogen oxidation experiment using catalyst bed 2, experiment 2.

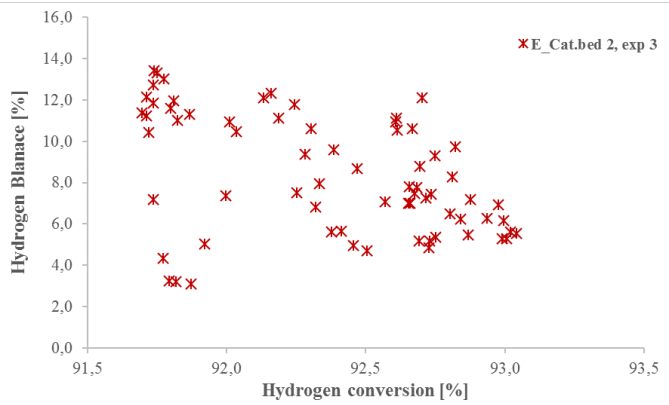

Figure D.7: Error in hydrogen mass balance plotted against hydrogen conversion in the hydrogen oxidation experiment using catalyst bed 2, experiment 3, duration of 3 days.

Table D.2: Temperatures trough the reactor at 20.5 cm axial position compared to the temperature set point for the carbon monoxide oxidation experiment catalyst bed 2, experiment 3, cooling cycle following the three day experiment. The catalyst bed is located at 19 - 21 cm.

Set point temperature [°C]	**Temperature at 20.5 cm axial position**
200	178
300	255
400	344
500	430
600	534
700	631

D.2 Carbon Monoxide Oxidation

Additional information and results from carbon monoxide oxidation experiments are shown in this section.

Temperature profiles over the catalyst bed were measured for each experiment to measure the temperature gradient and to control where the exothermic reactions are taking place. The profiles for the blank experiment and catalyst bed 2, experiments 1 - 3, are shown in Figures D.8 to D.10 and Table D.2.

The mass balance error for carbon was calculated for each carbon monoxide oxidation experiment to assess the accuracy of the GC analysis and is shown in Figures D.11 to D.13 for experiments using catalyst bed 2, experiments 1-3.

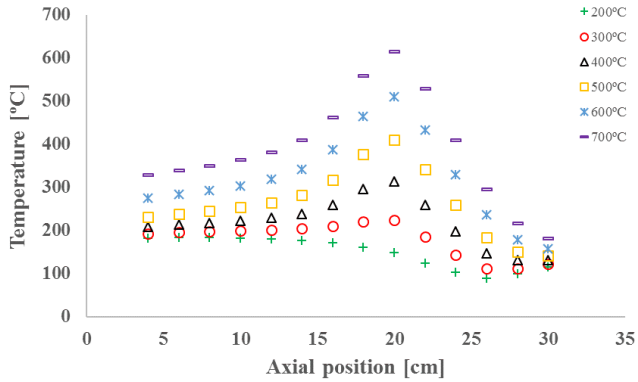

Figure D.8: Graph showing the temperature profile trough the reactor plotted against the axial position of the thermocouple in the blank carbon monoxide oxidation experiment. The catalyst bed would be located at 19 - 21 cm.

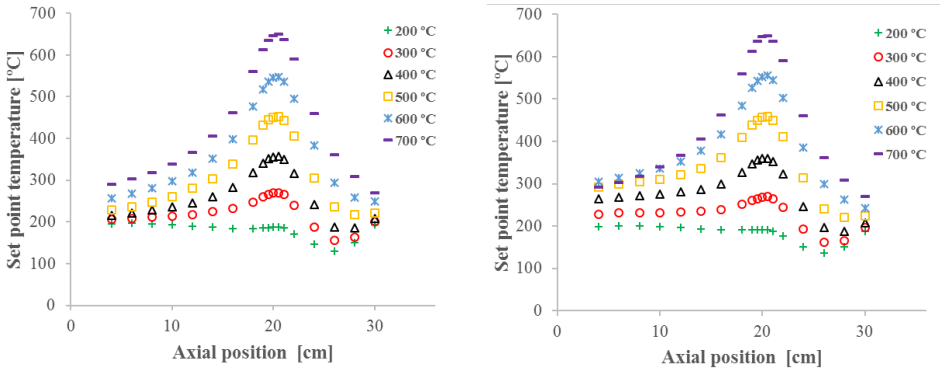

Figure D.9: Graph showing the temperature profile trough the reactor plotted against the axial position of the thermocouple in the carbon monoxide oxidation experiment catalyst bed 2, experiment 1, for reactor heating (a) and cooling (b) cycle. The catalyst bed is located at 19 - 21 cm.

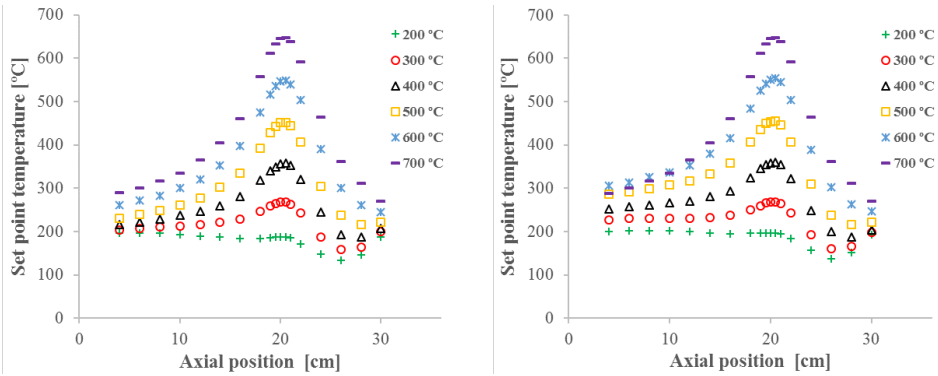

Figure D.10: Graph showing the temperature profile trough the reactor plotted against the axial position of the thermocouple in the carbon monoxide oxidation experiment catalyst bed 2, experiment 2, for reactor heating (a) and cooling (b) cycle. The catalyst bed is located at 19 - 21 cm.

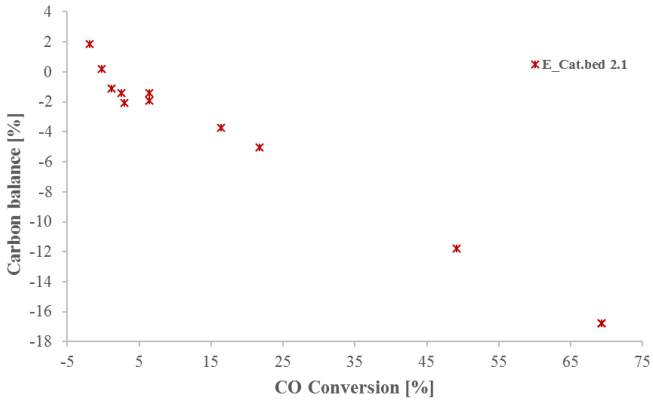

Figure D.11: Error in carbon mass balance plotted against CO conversion in the carbon monoxide oxidation experiment using catalyst bed 2, experiment 1.

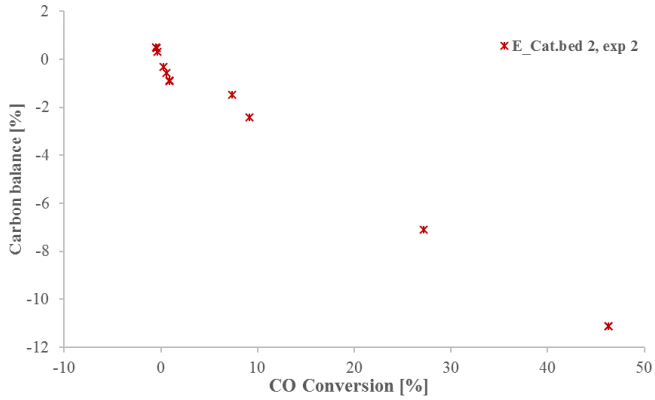

Figure D.12: Error in carbon mass balance plotted against CO conversion in the carbon monoxide oxidation experiment using catalyst bed 2, experiment 2.

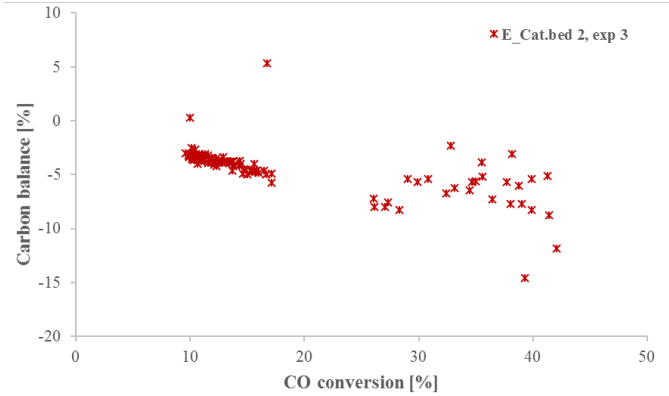

Figure D.13: Error in carbon mass balance plotted against CO conversion in the carbon monoxide oxidation experiment using catalyst bed 2, experiment 3, duration of 3 days.